A novel combined evolutionary algorithm for optimal planning of distributed generators in radial distribution systems

applied sciences

MDPI

Article

A Novel Combined Evolutionary Algorithm for Optimal Planning of Distributed Generators in Radial Distribution Systems

Rabea Jamil Mahfoud [1], Yonghui Sun [1,*], Nizar Faisal Alkayem [2], Hassan Haes Alhelou [3], Pierluigi Siano [4,*] and Miadreza Shafie-khah [5]

1 College of Energy and Electrical Engineering, Hohai University, Nanjing 210098, China
2 Department of Engineering Mechanics, Hohai University, Nanjing 210098, China
3 Department of Electrical Power Engineering, Faculty of Mechanical and Electrical Engineering, Tishreen University, Lattakia 2230, Syria
4 Department of Management & Innovation Systems, University of Salerno, 84084 Salerno, Italy
5 School of Technology and Innovations, University of Vaasa, 65200 Vaasa, Finland
* Correspondence: sunyonghui168@gmail.com (Y.S.); psiano@unisa.it (P.S.); Tel.: +39-320-4646-454 (P.S.)

Received: 7 July 2019; Accepted: 15 August 2019; Published: 17 August 2019

Abstract: In this paper, a novel, combined evolutionary algorithm for solving the optimal planning of distributed generators (OPDG) problem in radial distribution systems (RDSs) is proposed. This algorithm is developed by uniquely combining the original differential evolution algorithm (DE) with the search mechanism of Lévy flights (LF). Furthermore, the quasi-opposition based learning concept (QOBL) is applied to generate the initial population of the combined DELF. As a result, the new algorithm called the quasi-oppositional differential evolution Lévy flights algorithm (QODELFA) is presented. The proposed technique is utilized to solve the OPDG problem in RDSs by taking three objective functions (OFs) under consideration. Those OFs are the active power loss minimization, the voltage profile improvement, and the voltage stability enhancement. Different combinations of those three OFs are considered while satisfying several operational constraints. The robustness of the proposed QODELFA is tested and verified on the IEEE 33-bus, 69-bus, and 118-bus systems and the results are compared to other existing methods in the literature. The conducted comparisons show that the proposed algorithm outperforms many previous available methods and it is highly recommended as a robust and efficient technique for solving the OPDG problem.

Keywords: radial distribution systems; distributed generators; differential evolution; Lévy flights; quasi-opposition based learning

1. Introduction

The importance of the optimal operation of radial distribution systems (RDSs) arises from the continuous need of highly reliable operation of those systems to ensure high quality delivered-power to the end consumers, which is not an easy mission due to multiple reasons. The main reason is the lack of controllability because of the absence of power generation, in other words, the passive nature of RDSs. Other reasons are the high R/X ratio and the increase of load demand [1].

The operation of RDSs with the presence of those difficulties may lead to many operational problems, such as low reliability and bad quality of electricity, an increase of the system's power losses, high voltage deviation, and poor voltage stability. Converting the nature of RDSs from passive to active by installing small distributed generators (DG) near to end consumers is one of the solutions to overcome those technical problems. DG units improve the voltages along the feeder; enhance the reliability, as well as the quality; increase the voltage stability; allow more power to be transmitted

through the feeders which defers the investments on future expansion of transmission and distribution systems; and reduce the total system's losses along with their costs [2,3].

In order to extract the maximum advantages from the installed DGs, it is necessary to allocate them at the optimum buses with the optimal sizes, whereas inappropriate installation of DGs could lead to unwanted effects, such as higher power losses. Hence, the optimal planning of DGs (OPDG) is regarded as a critical problem needed to be effectively solved, especially for large-scale RDSs. It is difficult to find the global optimal solution of the OPDG problem, due to the nonlinear nature of the objective functions and constraints. Therefore, this challenge gives researchers a good motivation to develop new algorithms for solving this problem. In recent years, numerous research works using different methods have been published about the OPDG problem in RDSs. Those methods can be basically categorized into groups which are mainly: Analytical techniques, conventional approaches, and evolutionary algorithms [4,5].

Many analytical techniques have been applied for solving the OPDG problem in RDSs [6–10]. Some of them are based on sensitivity indices, such as power stability index [6], voltage stability index [7], and combined power loss sensitivity [8]. A comparison of optimal DG allocation methods based on many sensitivity approaches was presented in [9]. In [10], the proposed method was based on minimizing the losses associated with the changes in active and reactive components of branch currents caused by DG placements. In general, most of those analytical methods were applied to only minimize power loss in small and medium-scale RDSs.

The nonlinear features of the OPDG problem make it solvable by implementing the conventional iterative methods. Two of those methods are: Non-linear programming (NLP) [11], and dynamic programming (DP) [12]. In [13], the active power loss was minimized by a mixed integer non-linear programming (MINLP) based approach, which was used for allocating single and multiple DGs in RDSs. The main disadvantage of those methods was their inability when dealing with complex and large-scale problems, regarding either the computational time or convergence.

In the last few decades, evolutionary algorithms (EA) have been massively employed for solving the OPDG problem. Those metaheuristic methodologies have proved their ability to effectively solve that problem even for complex and large-scale RDSs. In [14], the OPDG was addressed as multi-objective mixed integer problem solved by a genetic algorithm (GA) used to minimize the costs of different parts of the system. Many versions of GAs were developed to deal with the OPDG problem, as in [15,16], where the power loss and voltage deviation were minimized by the optimal allocation of DGs, considering uncertainties of load and generation in [15]. The same objectives of power loss and voltage deviation were minimized by optimally allocating DGs and on-load tap changer (OLTC) in [16]. A particle swarm optimization (PSO) algorithm was also widely used for solving the OPDG problem. A multi-objective index-based method for the optimal planning of multiple DGs in RDSs with different loads was proposed in [17] by applying PSO. In [18], different types of DGs were considered for the optimal planning by minimizing the power loss using PSO. A new formulation was proposed to consider the uncertainties in the renewable DGs output in order to optimally allocate them while minimizing the total harmonic distortion, power loss, and total costs by PSO in [19]. An artificial bee colony (ABC) based method was presented in [20] to solve the OPDG problem by minimizing the power loss. Several algorithms were also developed to solve that problem, such as the modified honey bee mating optimization algorithm (HBMO) [21], the improved gravitational search algorithm (IGSA) [22], and symbiotic organisms search (SOS) algorithm [23].

Moreover, the hybridization of two or more EA methods in order to improve their performances has been rapidly adopted as an efficient way to solve the OPDG problem. The authors in [24] presented a hybrid GA–PSO method to simultaneously minimize the power loss and voltage deviation while enhancing the voltage stability. A multi-objective hybrid teaching—learning based optimization—Grey–Wolf optimizer (MOHTLBOGWO) based on a fuzzy decision-making method was developed in [25] for loss minimization and reliability enhancement using renewable DGs. Another multi-objective opposition based chaotic differential evolution (MOCDE) algorithm was proposed

in [26] for solving a similar problem but with various objectives. Additionally, powerful hybrid techniques were proposed to find the optimal solution of the same problem, such as the grid-based multi-objective harmony search (GrMHS) algorithm [27], and the quasi-oppositional swine influenza model based optimization with quarantine (QOSIMBO-Q) [28].

However, most of the aforementioned algorithms were only applied on small and medium-scale RDSs. Nevertheless, few works have been done so far considering the large-scale systems [29–32]. The algorithms applied in those papers are: QO-teaching-learning based optimization (QOTLBO) [29], loss sensitivity factor-simulated annealing (LSFSA) [30], krill herd algorithm (KHA) [31], and stochastic fractal search algorithm (SFSA) [32]. Therefore, new and robust algorithms are needed to solve the OPDG problem, especially for large-scale RDSs with different combinations of the most important objectives regarding the optimal operation of radial systems.

In this paper, a novel combined evolutionary algorithm, named the quasi-oppositional differential evolution Lévy flights algorithm (QODELFA) is proposed. The quasi-opposition based learning concept (QOBL) is applied to generate the initial population of the combination between the original differential evolution (DE) algorithm and the Lévy flights (LF) perturbation. The new method is utilized for optimal sitting and sizing of DGs in RDSs by taking three objective functions (OFs) under consideration. Those OFs are the active power loss (APL) minimization, the voltage deviation (VD) improvement, and the voltage stability index (VSI) enhancement. Two types of DGs are studied based on their power factor (PF); i.e., unity and non-unity. Different combinations of the three OFs are considered while satisfying several operational constraints. The effectiveness of the proposed QODELFA is tested and verified on the IEEE 33-bus, 69-bus, and large-scale 118-bus systems, and the results are compared to many existing methods in the literature.

The rest of this paper is arranged as follows: The detailed description of the proposed QODELFA is presented in Section 2. A performance comparison between QODELFA and several novel algorithms is also addressed in this section. The OPDG problem formulation is explained in Section 3. In Section 4, the implementation of the proposed algorithm on the OPDG problem is described in details. Simulation results, comparisons, and discussions are demonstrated in Section 5. Finally, Section 6 outlines the conclusions.

2. Details and Performance Analysis of QODELFA

2.1. Main Procedures of QODELFA

The QODELFA proposed in this paper is basically a unique combination of the DE algorithm and LF perturbation. Furthermore, the concept of QOBL is applied to generate the initial population of the combined DELFA. The main operations and steps of QODELFA are demonstrated in detail as follows.

2.1.1. Procedures of DE

DE is a simple and efficient meta-heuristic optimization method [33]. The basics of DE are described in this subsection.

- Mutation:

The concept of DE depends on generating new solutions by

$$Sl_{m_i} = Sl_{rnd_1} + F_{DE} \cdot (Sl_{rnd_2} - Sl_{rnd_3}) \quad (1)$$

where Sl_{m_i} stands for the mutant solution, Sl_{rnd_1}, Sl_{rnd_2}, and Sl_{rnd_3} are randomly defined solutions, and $F_{DE} \in [0, 2]$ is an amplifying parameter.

For better enhancing the DE's performance, the superior solution Sl_{su} is deduced in every generation, and multiple randomly defined solutions (Sl_{rnd_1}, Sl_{rnd_2}, Sl_{rnd_3}, and Sl_{rnd_4}) are created. This procedure can be explained as

$$Sl_{m_i} = Sl_{su} + F_{DE}^{m} \cdot (Sl_{rnd_1} - Sl_{rnd_2} + Sl_{rnd_3} - Sl_{rnd_4}), \tag{2}$$

where F_{DE}^{m} is modified by utilizing it as given in the following equation

$$F_{DE}^{m} = F_{\max} - (t-1)(F_{\max} - F_{\min})/(M-1), \tag{3}$$

where $F_{\min} = 0$, $F_{\max} = 2$, t is the iteration number, and M is the maximum number of iterations.

- Crossover:

Another improvement of the searching process is done by executing the crossover, where trial solutions tr_i in iteration $t+1$ are evolved by

$$tr_i^{t+1} = \begin{cases} Sl_{m_i}^{t+1} & if \quad r \le cr \\ Sl_i^t & if \quad r \ge cr \end{cases}, \tag{4}$$

where $r \in [0,1]$, and cr is the crossover rate.

- Greedy Selection:

The last step in DE is to perform the selection by the 'greedy selection', where a comparison between $Sl_{m_i}^{t+1}$ and Sl_i^t is made, then the most superior solution will be placed in the population.

2.1.2. LF Perturbation:

LF perturbation is based on mathematically characterizing the random walks of the critters [34], where the generation of a new solution by LF is executed by

$$Sl_i^{t+1} = Sl_i^t + step_i, \tag{5}$$

where $step_i$ is the step size [34], which is calculated by

$$step_i = \alpha_0 (Sl_j^t - Sl_i^t) \oplus Levy(\beta) \approx 0.01 \frac{x}{|y|^{\frac{1}{\beta}}} (Sl_j^t - Sl_i^t), \tag{6}$$

where α_0 is a constant, Sl_j^t and Sl_i^t stand for two randomly defined solutions, $\oplus$ is the entry-wise multiplication, $Levy(\beta)$ represents the Lévy probability distribution function of β, and x and y can be computed by applying the normal distribution function

$$\begin{cases} x = N(0, \sigma_x^2) \\ y = N(0, \sigma_y^2) \end{cases}, \tag{7}$$

where $\sigma_x = \left[\frac{\Gamma(1+\kappa)\sin(\frac{\pi\kappa}{2})}{\Gamma\left[\frac{(1+\kappa)}{2}\right]\kappa 2^{\frac{(\kappa-1)}{2}}} \right]^{\frac{1}{\eta}}$, $\kappa \in [1,2]$ is an index, Γ stands for the gamma function, $\eta = 1.5$ and $\sigma_y = 1$.

2.1.3. Concept of QOBL

The opposition-based learning (OBL) was essentially developed for the purpose of reducing the computational time, as well as improving the convergence abilities of different EAs [35]. By considering each of the current populations and their opposite populations based on OBL, the candidate solution

will be improved. This concept is simple and easy to implement which makes it suitable to enhance the performance of the combined DELF algorithm proposed in this paper. As mentioned in [35], an opposite candidate solution (CS) might be closer to the global optimal solution than an arbitrary CS. Hence, the comparison between a random CS and its opposite will lead to the global optimum with faster convergence rate. The quasi-opposite number was further investigated in [36] and proved that it is usually closer to the optimal solution than the opposite number. This improved concept of QOBL has been used to solve the OPDG problem by enhancing the performance of some algorithms [28,29], but it has not been utilized to improve such a combined DELF algorithm as proposed in this paper. Accordingly, the initial population of this algorithm is generated based on the QOBL concept, where the greedy selection of DE is employed to determine whether an initial random solution is better than its quasi-opposite solution or not. As a result of this comparison, the best among original and quasi-opposite solutions will be kept in the initial population. This will increase the diversity and exploration of the generated initial population. Consequently, the algorithm will mostly converge to the global optimum with faster rate. The definitions of opposite number, opposite point, quasi-opposite number, and quasi-opposite point are given as follows [28]:

For any random number $x \in [a, b]$, its opposite number x_o is given by

$$x_o = a + b - x, \tag{8}$$

while the opposite point for multi-dimensional search space (d dimensions) is defined as

$$x_o^i = a^i + b^i - x^i;\ i = 1, 2, \ldots, d \tag{9}$$

and the quasi-opposite number x_{qo} of any random number $x \in [a, b]$ is given by

$$x_{qo} = rand(\frac{a+b}{2}, x_o), \tag{10}$$

similarly, the quasi-opposite point for multi-dimensional search space (d dimensions) is defined as

$$x_{qo}^i = rand(\frac{a^i + b^i}{2}, x_o^i). \tag{11}$$

2.2. The QODELFA

The main procedures mentioned in the previous subsection are uniquely combined to construct the QODELFA as depicted in the flowchart given in Figure 1. The stochastic parameters of the proposed technique are varied in a step-wise fashion to select the optimal parameter values able to provide the best algorithmic performance. First, an initial population of random solutions is created and then enhanced by using the QOBL concept. Thereafter, the DE is used to improve the initial population using mutation, crossover and selection. After that, the LF perturbation is executed along with the DE's crossover and selection operations. The greedy selection is utilized as a selection mechanism along the stages of the algorithm. Finally, the iterations are terminated when the stopping criteria are satisfied.

2.3. Performance Comparison by Solving Benchmark Functions

In order to analyze the performance of QODELFA, ten benchmark functions taken from [37], as shown in Table 1, were used as test functions. Besides, the proposed algorithm's performance was compared with several algorithms: PSO, DE, GA, ABC, the sine-cosine algorithm (SCA), and the firefly algorithm (FA). The default parameters of those algorithms were used in this procedure. For each test function and each algorithm, ten independent runs are executed. For the comparison purposes, 40,000 evaluations were considered for all algorithms.

Table 2 illustrates the results for minimizing the test functions using the mentioned algorithms, including the minimum (Min.), maximum (Max.), mean, and standard deviation (SD) values for each function. The desired optimal value of minimizing all the ten benchmark functions is zero.

According to the results presented in Table 2, it can be observed that QODELFA gives better values than the other algorithms regarding most of the test functions. Those results verify the robustness of the proposed algorithm.

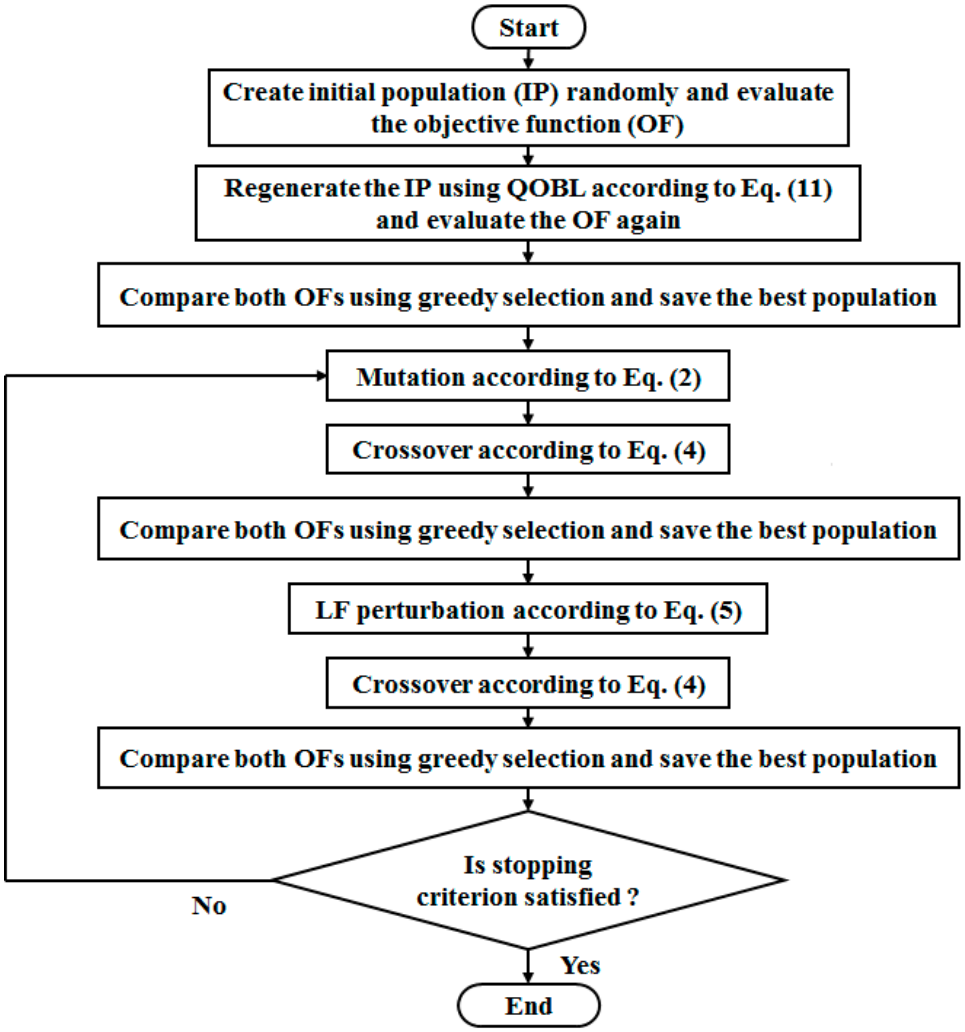

Figure 1. Flowchart of the quasi-oppositional differential evolution Lévy flights algorithm (QODELFA).

The effectiveness of QODELFA was further validated by comparing its convergence characteristics with those of the algorithms listed in Table 2. The functions: Rastrigin, Perm $0, d, \beta$, Power sum, and Rosenbrock were selected for this test as they are categorized in different groups [37]. A total of 20,000 evaluations were considered for all algorithms in this comparison. Figures 2–5 illustrate the evolution of the mean value of the four functions versus the iteration number of all algorithms. The "semiology" command is used in Matlab for plotting, since the logarithmic scale on the y-axis is needed to clearly depict the comparison. As obviously shown in Figures 2–5, the QODELFA effectively converges to the optimal values faster than the other algorithms.

3. OPDG Problem Formulation

The aim of the OPDG problem studied in this paper is to optimally allocate and operate DGs in RDSs to minimize each instance of active power loss and voltage deviation, and maximize the voltage stability index, while satisfying different equality and inequality constraints.

The mathematical formulations of this optimization problem are given as follows.

3.1. Objective Functions

3.1.1. Minimization of Active Power Loss

The active power loss (APL) of the RDS is minimized according to this objective function which is given by

$$OF_1 : \min(\frac{APL}{APL_b}), \tag{12}$$

where APL_b is the active power loss of the base-case (before adding DGs). The APL is expressed by

$$APL = \sum_{k=1}^{br} I_k^2 R_k, \tag{13}$$

where br is the number of branches in the system, and I_k and R_k are the current and resistance of branch k, respectively [25].

Table 1. Benchmark functions.

Function	Formula	Input Domain	No. of Parameters
$f_1(x)^1$	$-20\exp\left(-0.2\sqrt{\frac{1}{d}\sum_{i=1}^{d}x_i^2}\right)-\exp\left(\frac{1}{d}\sum_{i=1}^{d}\cos(2\pi x_i)\right)+20+e$	[−32.768,32.768]	20
$f_2(x)^2$	$\sum_{i=1}^{d}\frac{x_i^2}{4000}-\prod_{i=1}^{d}\cos\left(\frac{x_i}{\sqrt{i}}\right)+1$	[−600,600]	20
$f_3(x)^3$	$10d+\sum_{i=1}^{d}\left[x_i^2-10\cos(2\pi x_i)\right]$	[−5.12,5.12]	5
$f_4(x)^4$	$\sin^2(\pi w_1)+\sum_{i=1}^{d-1}(w_i-1)^2\left[1+10\sin^2(\pi w_i+1)\right]+(w_d-1)^2\left[1+\sin^2(2\pi w_d)\right]$	[−10,10]	20
$f_5(x)^5$	$\sum_{i=1}^{d}\left(\sum_{j=1}^{d}(j+\beta)\left(x_j^i-\frac{1}{j^i}\right)\right)^2$	[−d,d]	5
$f_6(x)^6$	$\sum_{i=1}^{d}ix_i^2$	[−10,10]	30
$f_7(x)^7$	$\sum_{i=1}^{d}\sum_{j=1}^{i}x_j^2$	[−65.54,65.54]	20
$f_8(x)^8$	$\sum_{i=1}^{d}\left[\left(\sum_{j=1}^{d}x_j^i\right)-b_i\right]^2$	[0,d]	4
$f_9(x)^9$	$\sum_{i=1}^{d-1}\left[100(x_{i+1}-x_i^2)^2+(x_i-1)^2\right]$	[−5,10]	4
$f_{10}(x)^{10}$	$(x_1-1)^2+\sum_{i=2}^{d}i(2x_i^2-x_{i-1})^2$	[−10,10]	10

[1]Ackley, [2]Griewank, [3]Rastrigin, [4]Levy, [5]Perm $0,d,\beta$, [6]sum squares, [7]rotated hyper-ellipsoid, [8]power sum, [9]Rosenbrock, [10]Dixon–Price.

3.1.2. Minimization of Voltage Deviation

The voltage deviation (VD) of the system is minimized based on this objective function so that the voltage profile is improved, which is given by

$$OF_2 : \min(\frac{VD}{VD_b}), \tag{14}$$

where VD_b is the voltage deviation of the base-case. The VD is formulated as

$$VD = \sum_{i=1}^{n} (V_i - V_r)^2, \tag{15}$$

where n denotes the number of buses in the system, V_i is the voltage magnitude at bus i, and V_r is the rated voltage which is equal to 1.0 p.u. [24].

3.1.3. Maximization of Voltage Stability Index

As shown in Figure 6, the voltage stability index (VSI) of bus $j = 2, 3, \ldots, n$ of an RDS is defined by

$$VSI_j = |V_i|^4 - 4 * (P_j X_k - Q_j R_k)^2 - 4 * (P_j R_k + Q_j X_k) * |V_i|^2. \tag{16}$$

The VSI is usually calculated to evaluate whether the system is stable or not, where for stable systems, VSI should be more than zero for all buses along the feeder so that the system can avoid the voltage collapse. Thus, this index needs to be maximized [25]. In this case, the objective function is written as

Table 2. Comparison of results for minimizing benchmark functions by using different algorithms.

Function	Value	GA	PSO	DE	FA	ABC	SCA	QODELFA
$f_1(x)$	Min.	0.001500000	**7.9936E-15**	5.5078E-05	3.5994E-05	0.001499	3.3672E-05	3.2346E-06
	Max.	1.501800000	**1.5099E-14**	9.1151E-05	5.0207E-05	0.005632	0.00136427	1.8930E-05
	Mean	0.494010000	**1.1546E-14**	7.7296E-05	4.3945E-05	0.003136	0.00052707	7.6498E-06
	SD	0.650915210	**3.7449E-15**	1.3982E-05	4.1056E-06	0.001235	0.00039639	4.6941E-06
$f_2(x)$	Min.	1.67057E-07	1.85E-13	1.89310E-06	4.48524E-08	0.023929	3.53044E-05	**3.01981E-14**
	Max.	0.007396679	0.058921	6.47944E-05	0.009864731	0.305490	0.260080741	**0.022126734**
	Mean	0.000740400	0.026802	1.42411E-05	0.002465738	0.088867	0.079647319	**0.007140086**
	SD	0.002338778	0.019734	1.85757E-05	0.004026563	0.085039	0.105481599	**0.008401261**
$f_3(x)$	Min.	0.994959	0	2.01E-11	0.994959	0.200500	0	**0**
	Max.	5.969749	1.989918	1.15E-09	5.969754	1.657200	9.32E-11	**3.34E-13**
	Mean	2.984877	0.596975	3.80E-10	3.283365	0.768219	9.40E-12	**1.19E-13**
	SD	1.483196	0.839023	3.53E-10	1.410988	0.537652	2.94E-11	**1.23E-13**
$f_4(x)$	Min.	3.02E-09	**3.28E-19**	6.41E-10	9.21E-11	0.000138	1.056931	1.80E-12
	Max.	0.998176	**3.91E-18**	2.03E-09	1.33E-10	0.001058	1.279176	4.79E-10
	Mean	0.172109	**2.65E-18**	1.14E-09	1.19E-10	0.000406	1.180877	9.38E-11
	SD	0.335319	**1.52E-18**	4.79E-10	1.27E-11	0.000265	0.085863	1.45E-10
$f_5(x)$	Min.	0.000224	3.50E-05	0.003839	8.36E-09	0.001526	0.204203	**8.50E-11**
	Max.	0.051547	0.000233	0.105156	0.031277	0.025481	1.154009	**1.91E-09**
	Mean	0.017779	0.000159	0.031891	0.005996	0.014717	0.523433	**7.76E-10**
	SD	0.018239	7.25E-05	0.030668	0.009571	0.008200	0.299470	**5.70E-10**
$f_6(x)$	Min.	1.50E-05	**5.76E-13**	6.34E-05	7.05E-09	0.119930	0.001221	4.21E-06
	Max.	0.000791	**3.05E-11**	0.000117	1.08E-08	0.221020	2.772696	9.49E-05
	Mean	0.000243	**8.88E-12**	9.21E-05	9.15E-09	0.169986	0.887205	3.10E-05
	SD	0.000294	**9.99E-12**	1.57E-05	1.02E-09	0.032625	1.029825	2.83E-05
$f_7(x)$	Min.	2.91E-08	**2.22E-17**	1.13E-07	7.16E-08	6.58E-05	1.14E-06	1.19E-09
	Max.	0.002864	**5.91E-15**	2.52E-07	1.09E-07	0.000191	0.001364	6.48E-08
	Mean	0.000306	**1.21E-15**	1.84E-07	9.21E-08	0.000109	0.000251	1.87E-08
	SD	0.000900	**1.93E-15**	3.93E-08	1.36E-08	3.71E-05	0.000455	2.12E-08
$f_8(x)$	Min.	0.000104	3.97E-09	0.001110	6.21E-08	0.002016	0.068476	**1.36E-11**
	Max.	0.067100	0.000751	0.035307	0.000303	0.024256	1.294515	**4.61E-07**
	Mean	0.012986	0.000230	0.016135	0.09E-07	0.009848	0.832464	**8.88E-08**
	SD	0.021051	0.000288	0.012371	0.000102	0.007333	0.404648	**1.34E-07**
$f_9(x)$	Min.	0.044047	0.002463	0.003089	1.01E-11	0.004665	0.389459	**0**
	Max.	3.750229	0.007062	0.068908	8.66E-11	0.146660	1.238042	**3.72E-29**
	Mean	1.217668	0.004882	0.023161	4.15E-11	0.052185	0.694527	**5.08E-30**
	SD	1.364193	0.001598	0.022713	2.45E-11	0.041106	0.247694	**1.16E-29**
$f_{10}(x)$	Min.	0.666667	1.84E-12	1.19E-11	0.666667	0.592410	0.666668	**0.028088**
	Max.	0.666747	0.666667	0.743694	0.666667	0.667160	0.666776	**0.097842**
	Mean	0.666675	0.600000	0.572044	0.666667	0.659358	0.666689	**0.058687**
	SD	2.54E-05	0.210819	0.302020	3.24E-11	0.023524	3.59E-05	**0.026335**

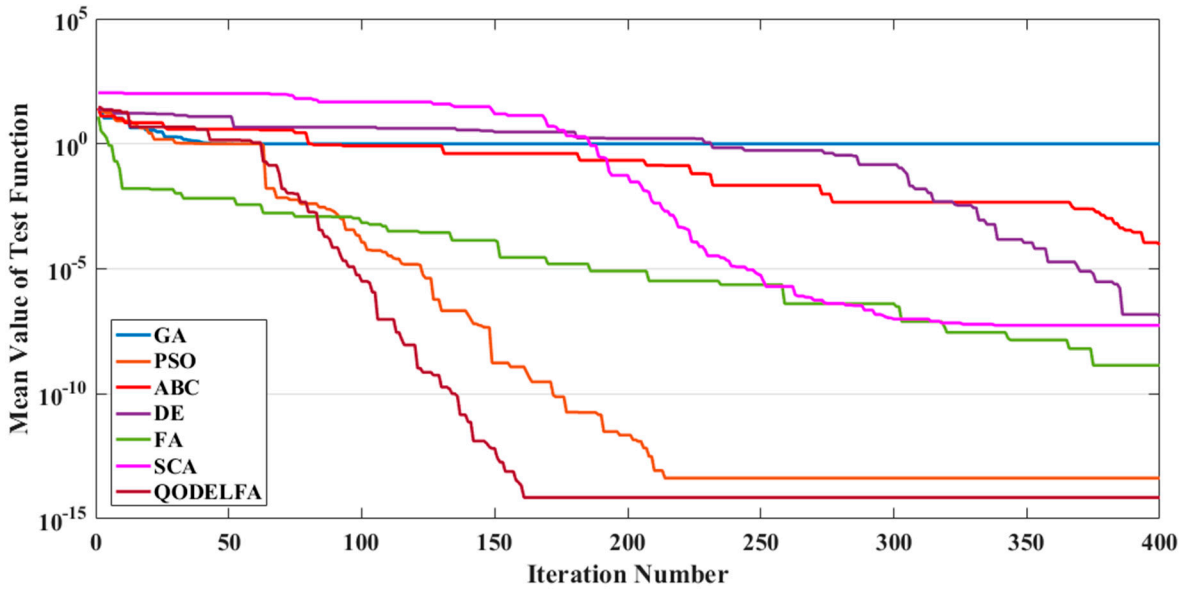

Figure 2. Convergence characteristics for Rastrigin function.

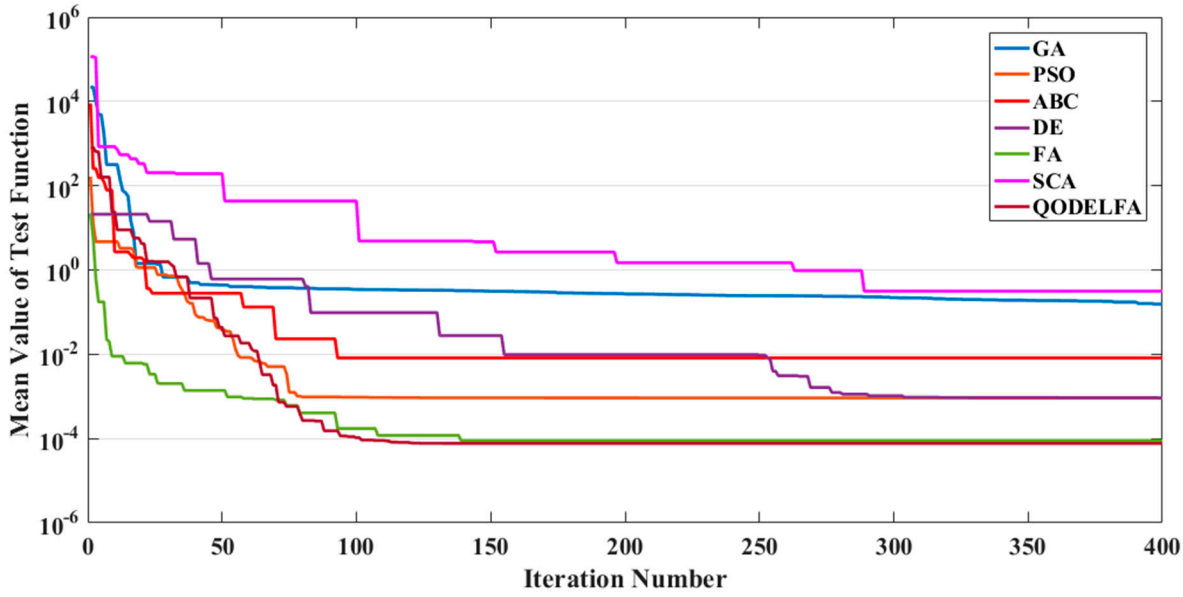

Figure 3. Convergence characteristics for Perm function $0, d, \beta$.

$$\max(VSI_j) = \min(\frac{1}{VSI_j}) \tag{17}$$

$$\Rightarrow OF_3 : \min(\frac{VSI^{-1}}{{VSI_b}^{-1}}), \tag{18}$$

where ${VSI_b}^{-1}$ is the voltage stability index of the base-case.

The overall objective function is formulated using the weighted sum method as follows:

$$F = \min(\omega_1 \cdot OF_1 + \omega_2 \cdot OF_2 + \omega_3 \cdot OF_3), \tag{19}$$

where ω_1, ω_2 and $\omega_3 \in [0, 1]$ are the weighting factors. In this paper, three different cases regarding the mentioned OFs are considered in the study according to their importance. Hence, for each case, the weighting factors will take different values, which will be explained later.

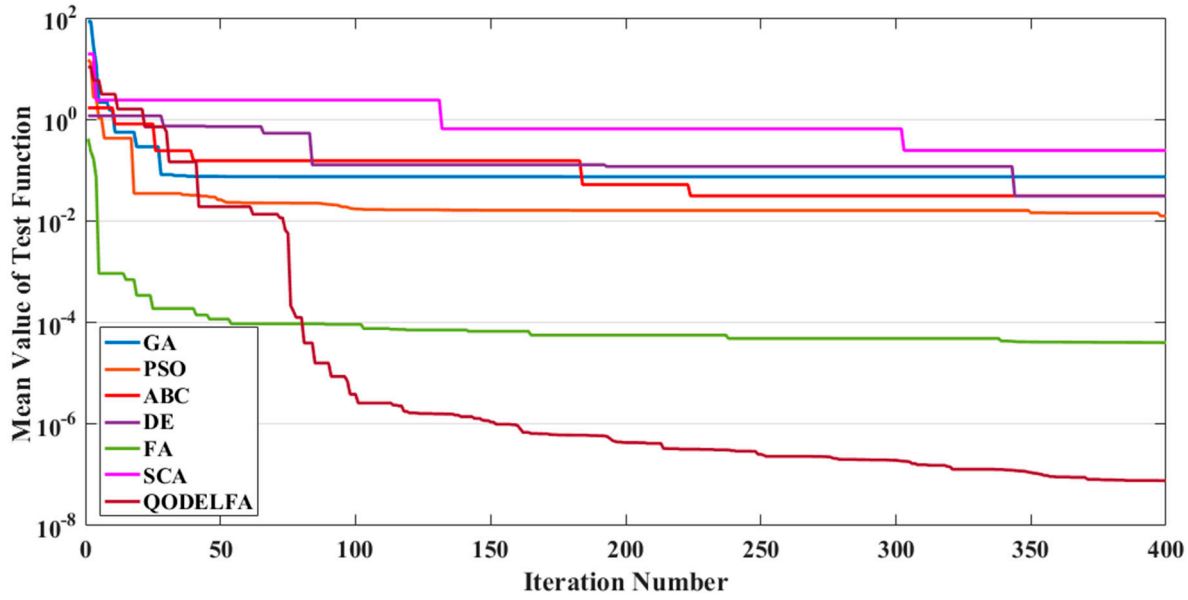

Figure 4. Convergence characteristics for the power sum function.

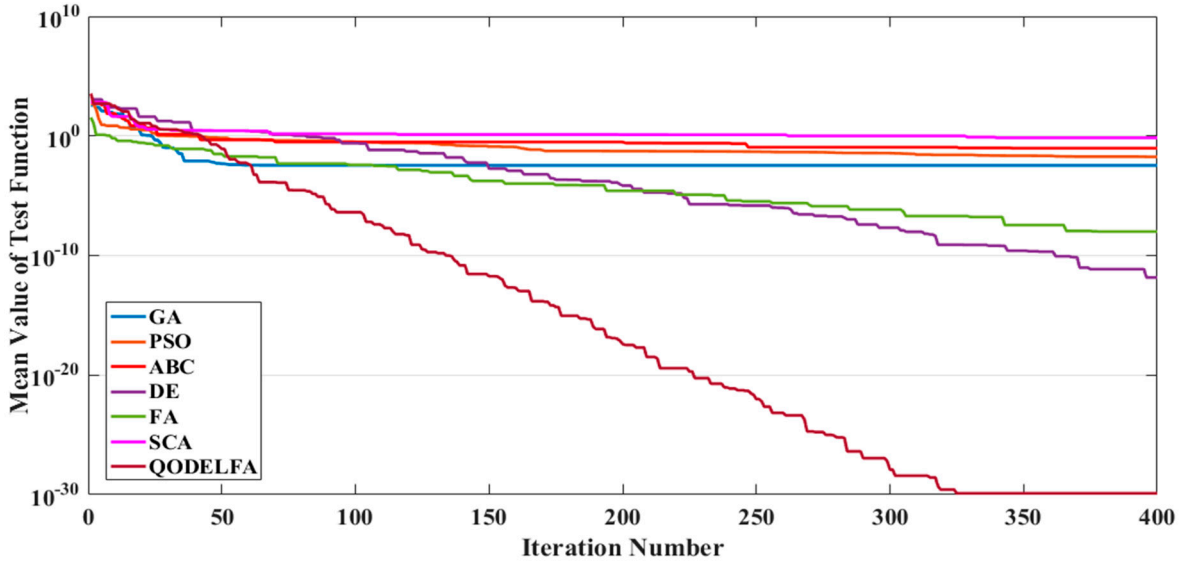

Figure 5. Convergence characteristics for the Rosenbrock function.

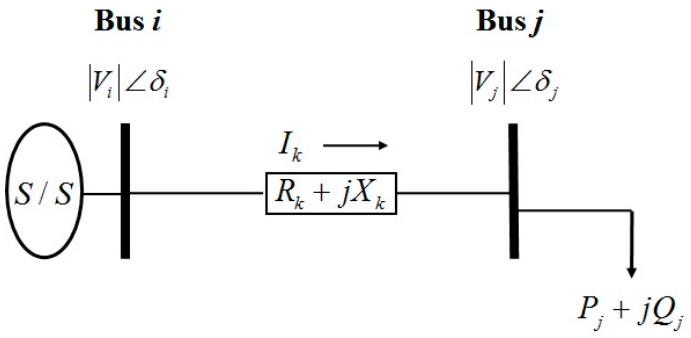

Figure 6. Equivalent circuit of a radical distribution system (RDS).

3.2. Constraints

3.2.1. Power Balance

The mathematical formulations of the power flow equations, which are defined as equality constraints are given by

$$P_{ss} + \sum_{i=1}^{n_{DG}} P_{DG_i} = \sum_{i=1}^{n_L} P_{L_i} + APL, \tag{20}$$

$$Q_{ss} + \sum_{i=1}^{n_{DG}} Q_{DG_i} = \sum_{i=1}^{n_L} Q_{L_i} + RPL, \tag{21}$$

where P_{ss} and Q_{ss} are the active and reactive power taken from the substation, P_{DG_i} and Q_{DG_i} are the active and reactive power of the DG at bus i, P_{L_i} and Q_{L_i} denote the active and reactive power of load at bus i, n_{DG} is the total number of DGs, n_L is the total number of loads, and APL and RPL represent the active and reactive power loss of the system, respectively [23].

3.2.2. Voltage Limits

The voltage magnitudes at all buses along the feeder should remain within the limits:

$$V_{\min} \leq V_i \leq V_{\max}, \tag{22}$$

where $V_{\max}$ and $V_{\min}$ are the upper and lower limits of bus voltage, respectively [27].

3.2.3. Active and Reactive Power Limits of DG

Both active and reactive powers of DGs should be kept in their limits as

$$P_{DG\min} \leq P_{DG_i} \leq P_{DG\max}, \tag{23}$$

$$P_{DG_i}^2 + Q_{DG_i}^2 \leq S_{DG_i}^2, \tag{24}$$

where $P_{DG\min}$ and $P_{DG\max}$ are the minimum and maximum limits of DG's active power, and P_{DG_i}, Q_{DG_i}, and S_{DG_i} denote the active, reactive, and apparent power of the DG at bus i, respectively [28].

It should be noted that for DGs at the unity power factor, only the constraint given in Equation (23) is considered. Whereas both constraints given in Equations (23) and (24) are taken when DGs operate at non-unity power factor.

3.2.4. Permissible Limit of DG Penetration

The sum of all powers injected into the system by DGs should be limited for unity power factor units as

$$\sum_{i=1}^{n_{DG}} P_{DG_i} \leq \sum_{i=1}^{n_L} P_{L_i}, \tag{25}$$

and for non-unity power factor units as

$$\sum_{i=1}^{n_{DG}} S_{DG_i} \leq \sum_{i=1}^{n_L} S_{L_i} \tag{26}$$

where S_{L_i} is the apparent power of load at bus i [32].

4. Implementation of QODELFA on the OPDG Problem

In this section, a detailed demonstration of utilizing the QODELFA to solve the OPDG problem in RDS by minimizing the APL, VD, and maximizing the VSI is given.

Algorithm: QODELFA for solving the OPDG problem.

A: Input load and line data for the RDS, and set required parameters for the algorithm: maximum number of iterations (M), population size (PS), total number of variables (N), cr, and β.
B: Run the power flow program to record the base-case values of the system's characteristics and the objective functions.
C: QOBL Initialization
1: Create initial population (IP) of random solutions by generating a (PS × N) matrix, where every row of this matrix contains the sizes and locations of DGs.
2: Evaluate the IP by the objective function (OF) given in (19) after adding penalties in case of violating the constraints as

$$OF_{Total} = OF + \rho_1 \sum_{i=1}^{n} (V_i - V_r)^2 + \rho_2 \sum_{i=1}^{n} (P_{DG} - P_{DG}^{\lim})^2 \quad (27)$$

where ρ_1, ρ_2 are penalty coefficients.
3: Regenerate the IP based on the QOBL technique given in (11).
4: Evaluate the QOBL-based IP by the OF_{Total} given in (27).
5: Apply the greedy selection (GS) to compare both IPs evaluated in steps 2 and 4 and save the best population.
6: Assign the QOBL-based population saved in step 5 as the IP of the DELF's main loop.
D: Main loop:
7: **while** stopping criterion is not satisfied, **do**
8: Apply the mutation of DE on the population according to (2) considering the limits on sizes and locations of DGs.
9: Evaluate the mutant solution by the OF_{Total} given in (27).
10: Execute the crossover on the mutant solution according to (4), then evaluate it by the OF_{Total} given in (27).
11: Apply the GS to keep the superior population by comparing both solutions evaluated in steps 9 and 10.
12: Apply the LF perturbation on the superior solution saved in step 11 according to (5) considering the limits on sizes and locations of DGs.
13: Evaluate the new solution by the OF_{Total} given in (27).
14: perform the crossover on the new solution according to (4), then evaluate it by the OF_{Total} given in (27).
15: Apply the GS to keep the new superior solution by comparing both solutions evaluated in steps 13 and 14.
16: **end while**
E: Display the final obtained solutions and save the results.

Remark 1: The QOBL technique has been used to solve the OPDG problem by enhancing the performance of some algorithms in the population initialization and generation stage as in [28,29], but this concept has not been utilized to improve a combined DELF algorithm, as proposed in this paper.

Remark 2: In general, evolutionary computation techniques initially depend on the generation of arbitrary solutions using Gaussian distribution functions. Thereafter, the preliminary solutions are improved by various operators to get the overall optimal or near optimal solutions. The proposed QODELFA applies two main frameworks; the former finds the global optimum solution using DE, whereas, the latter implements a local permutation using LF. Comparing it to the original DE algorithm previously applied for balanced systems [38], the implementation of QODELFA ensures the convergence towards the optimum rapidly and reliably. The combined technique also elects the elite solutions in each generation which guarantees the flexible flow of solutions to the optimal region inside the search space. The developed paradigm combining the above superior features is also suitable to be utilized in various engineering applications.

5. Results and Discussions

The QODELFA has been applied on three test systems: The IEEE-33 bus, 69-bus, and large-scale 118-bus systems. Backward-forward sweep algorithm (BFSA) has been used to run the load flow. For each system, three different cases were taken under consideration for the best verification and validity of the proposed algorithm. Case 1 represents the minimization of the system's APL, the minimization of both APL and VD together is addressed in Case 2, and Case 3 is for simultaneously minimizing APL, VD, and VSI^{-1}. Moreover, for each case, three subcases are tested depending on the power factor value of the DGs; i.e., with unity power factor, and with two different values of power factors.

Based on the literature included in this paper, and as mentioned in [18], different types of DGs can be characterized when they are optimally planned in radial distribution systems (RDSs). Those types can be distinguished depending on their capability of injecting active, reactive, or both active and reactive powers. The photovoltaic and fuel cells are good examples of DGs capable of injecting active power only, which means that they operate at a unity power factor. While synchronous machines are an example of DGs capable of injecting both active and reactive power, that means they operate at a non-unity power factor. Furthermore, different fixed power factors will lead to different operations and utilizations of DGs in RDSs. Thus, as observed in several references used for comparisons in this paper, such as [28,29,31,32,39], many types of DGs with unity and non-unity power factors are usually selected to simulate several categories of practical generators allocated in RDSs. Hence, it is

important to compare the proposed algorithm's performance with as many algorithms in the literature as possible, and to demonstrate the effect of selecting the best power factor value on achieving the optimal objective functions' values. Therefore, three different power factors are chosen for each case.

As it is observed from the literature survey, the concept of "better compromise among the objectives" has been used in many references when comparing results, especially for bi-objective and multi-objective optimization problems. Those objectives' importance- and value-wise comparisons are needed when the solutions obtained from any proposed method have one of a total of two objectives or two of a total of three objectives better or worse than the other solutions. Thus, all the comparisons performed in this paper have been done relying on this concept. As it is well known regarding the OPDG problem, the minimization of the system's APL is considered as the most important objective, as it has the biggest effect on the system's operation and performance. Therefore, the APL is usually given the highest significance in bi-objective and multi-objective optimization problems. Furthermore, the minimization of VD and VSI^{-1} contribute to enhancing the voltage profile and stability along the distribution feeder. Additionally, they serve to keep the minimum bus voltages within their limits as defined by the system's operators, which is also provided when minimizing the APL. In conclusion, when the APL value of the proposed algorithm is much better than that of another method, and the VD value of the proposed algorithm is slightly higher than that of the other method, also when the solutions obtained from the proposed method have two of the total three objectives better than the others, the proposed method's solutions will be regarded as better solutions due to the better compromise among the objectives.

Depending on the system's scale, the main QODELFA's parameters are defined, as mentioned before, using a step-wise variation of stochastic parameters in order to obtain the best performance of the algorithm, where cr is varied between 0 and 1 with a step of 0.1, and β is varied between 1.2 and 1.8 with step of 0.1. For each system and each case, 20 independent runs are performed to get the best solutions. Matlab-R2013a has been used for programming and running the codes on a PC with Intel Core processor (TM) i5, 3.2 GHz speed and 4 GB RAM.

5.1. System 1: The IEEE 33-Bus

The load and line data of this RDS are taken from [40]. The base voltage and power are 12.66 kV and 100 MVA. The total active and reactive power loads are 3.715 MW and 2.300 MVAr, respectively. The base-case active and reactive power losses obtained from solving the BFSA-based load flow are 210.99 kW and 143.13 kVAr, respectively.

The base-case values of the VD and (VSI^{-1}, VSI) are 0.13381 p.u. and (1.4988, 0.6672) p.u., respectively. For this system, the QODELFA's optimal parameters are selected as $PS = 50$, $cr = 0.9$, and $\beta = 1.7$ for all cases with $M = 200$.

5.1.1. Case 1: APL Minimization

In this case, only the APL minimization (OF_1) is considered. Hence, the weighting factors in Equation (18) are taken as $\omega_1 = 1, \omega_2 = \omega_3 = 0$. The QODELFA is applied for three different values of power factor: Unity, 0.95 and 0.866 lag. The results are listed in Table 3.

It can be noticed that the active power loss is reduced from the base-case value (210.988 kW) to 72.785 kW with unity power factor DGs (Case 1.1) by using the proposed algorithm. As shown in Table 3, the value of APL obtained from QODELFA is better than those from other methods in [13] and [28]. Although the results of QODELFA and SFSA applied in [32] are the same, but the DG sizes are smaller when using the algorithm evolved is this paper. When the power factor is set to 0.95 lag (Case 1 and 2), the APL is more effectively minimized by using QODELFA, where it reaches 28.533 kW. This value is better than that from SIMBO-Q algorithm [28], the same as that from SFSA [32], and approximately similar to that from QOSIMBO-Q algorithm [28]. When the power factor is set to 0.866 lag (Case 1.3), the loss reduction (LR) percentage reaches 92.73%, which is clearly higher than that from KHA [31]. This LR percentage explains the power factor's effect on decreasing the losses.

Table 3. Results for the IEEE 33-bus RDS with active power loss (APL) minimization (objective function 1, (OF_1)).

Technique	Optimal Locations	Optimal Sizes (MW/MVAr)	APL (kW)	VD (p.u.)	VSI^{-1} (p.u.)	VSI (p.u.)	LR%	SD
Case 1.1: DGs with unity power factor (PF = 1)								
SIMBO-Q [28]	14 24 29	0.7638/0.0 1.0415/0.0 1.1352/0.0	73.40	0.0151	1.1444	0.8738	65.21	-
QOSIMBO-Q [28]	14 24 30	0.7708/0.0 1.0965/0.0 1.0655/0.0	72.80	0.0151	1.1358	0.8804	65.50	-
MINLP [13]	13 24 30	0.8000/0.0 1.0900/0.0 1.0500/0.0	72.79	-	-	-	65.34	-
SFSA [32]	13 24 30	0.8020/0.0 1.0920/0.0 1.0537/0.0	72.785	0.01509	1.1357	0.8805	65.50	5.91E-09
QODELFA	**13** **24** **30**	**0.8018/0.0** **1.0913/0.0** **1.0536/0.0**	**72.785**	**0.01509**	**1.1358**	**0.8804**	**65.50**	**4.84E-08**
Case 1.2: DGs with lagging power factor (PF = 0.95)								
SIMBO-Q [28]	13 24 30	0.8875/0.2917 1.0853/0.3567 1.3092/0.4303	29.00	0.00098	1.0367	0.9646	86.26	-
QOSIMBO-Q [28]	13 24 30	0.8303/0.2729 1.1239/0.3694 1.2398/0.4075	28.500	0.00210	1.0493	0.9530	86.49	-
SFSA [32]	13 24 30	0.8306/0.2730 1.1256/0.3700 1.2396/0.4074	28.533	0.00207	1.0493	0.9530	86.48	5.24E-08
QODELFA	**13** **24** **30**	**0.8302/0.2728** **1.1247/0.3697** **1.2396/0.4074**	**28.533**	**0.00207**	**1.0493**	**0.9530**	**86.48**	**4.95E-07**
Case 1.3: DGs with lagging power factor (PF = 0.866)								
KHA [31]	13 24 30	0.8530/0.4925 0.9000/0.5196 0.8999/0.5196	19.578	-	1.0769	0.9286	90.72	-
QODELFA	**13** **24** **30**	**0.7582/0.4378** **1.0273/0.5930** **1.2139/0.7009**	**15.347**	**0.00065**	**1.0317**	**0.9692**	**92.73**	**5.82E-07**

The sign "-" means unreported.

After results evaluation, it is observed that the APL obtained from the proposed QODELFA for this case is better than the APLs from most of the available algorithms in the literature.

In addition, as indicated in Table 3, the SD of results in all cases when using the proposed algorithm is quite small, which proves its robustness.

It can be noted from the convergence characteristics of QODELFA given in Figure 7 that the proposed algorithm can quickly reach the optimal solutions for all cases (1.1, 1.2, and 1.3), which verifies its effectiveness.

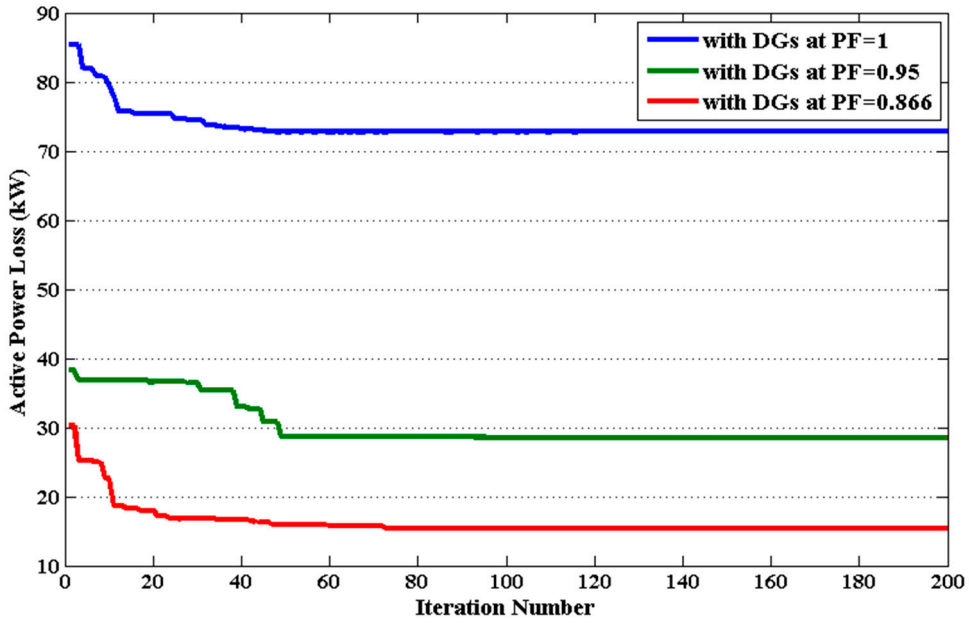

Figure 7. Convergence characteristics for Case 1 of the IEEE 33-bus system using QODELFA.

5.1.2. Case 2: Simultaneous Minimization of APL and VD

In this case, the minimization of both APL (OF_1) and VD (OF_2) is simultaneously considered. Therefore, in order to provide different solutions regarding the studied problem, the weighting factors in Equation (18) are taken as $\omega_1 = 0.5 = \omega_2 = 0.5, \omega_3 = 0$.

The QODELFA is applied for three different values of power factor: Unity, 0.95 and 0.866 lag. The results obtained by applying the proposed QODELFA are given in Table 4 and compared to those from two other methods. It might be noticed that, with unity power factor DGs (Case 2.1), the APL is reduced to 78.308 kW by using QODELFA, which is less than that of 92.50 kW from SIMBO-Q [28] and 88.90 kW from QOSIMBO-Q [28].

Similarly, when the power factor is set to 0.95 lag (Case 2.2), the APL reduced by QODELFA (29.231 kW) is lower than that of 32.20 kW from SIMBO-Q [28] and 31.10 kW from QOSIMBO-Q [28].

Since the VD values (0.0055 and 0.0007 p.u.) obtained by QODELFA are slightly higher than those obtained from both algorithms in [28], and the APL values (in kW) gained by QODELFA are much lower than those from the algorithms in [28] for cases 2.1 and 2.2, the solutions for both APL and VD of the proposed algorithm are regarded as better solutions because they have a better compromise than those of the methods from [28].

When the power factor is set to 0.866 lag (Case 2.3), the APL and VD reach 15.502 kW and 0.0003 p.u., respectively. This explains the power factor's effect again on the optimal operation of DGs as well as its importance to achieve better values of the studied objective functions. Moreover, as pointed out in Table 4, the very small SD of results in all cases obtained by the proposed algorithm also proves its robustness.

As noticed from Figure 8, which shows the convergence characteristics of Case 2 as a verification of effectiveness, the QODELFA can rapidly converge to the optimal solutions.

Table 4. Results for the IEEE 33-bus RDS with simultaneous minimization of OF_1 and OF_2.

Technique	Optimal Locations	Optimal Sizes (MW/MVAr)	APL (kW)	VD (p.u.)	VSI^{-1} (p.u.)	VSI (p.u.)	LR%	SD
Case 2.1: DGs with unity power factor (PF = 1)								
SIMBO-Q [28]	14 26 31	0.9029/0.0 1.4491/0.0 0.9137/0.0	92.50	0.0022	-	-	56.16	-
QOSIMBO-Q [28]	12 24 30	1.3232/0.0 1.0223/0.0 1.3735/0.0	88.90	0.0022	-	-	57.87	-
QODELFA	**13** **24** **30**	**1.0204/0.0** **1.1504/0.0** **1.2702/0.0**	**78.308**	**0.0055**	**1.0900**	**0.9175**	**62.88**	**3.45E-10**
Case 2.2: DGs with lagging power factor (PF = 0.95)								
SIMBO-Q [28]	13 24 30	0.8813/0.2897 1.3048/0.4289 1.5000/0.4930	32.20	0.0003	-	-	84.74	-
QOSIMBO-Q [28]	13 24 30	0.8303/0.2729 1.1239/0.3694 1.2398/0.4075	31.10	0.0003	-	-	85.26	-
QODELFA	**13** **24** **30**	**0.9001/0.2958** **1.1438/0.3759** **1.3214/0.4343**	**29.231**	**0.0007**	**1.0331**	**0.9679**	**86.48**	**4.13E-08**
Case 2.3: DGs with lagging power factor (PF = 0.866)								
QODELFA	**13** **24** **30**	**0.7582/0.4378** **1.0273/0.5930** **1.2139/0.7009**	**15.502**	**0.0003**	**1.0243**	**0.9763**	**92.65**	**3.71E-08**

The sign "-" means unreported.

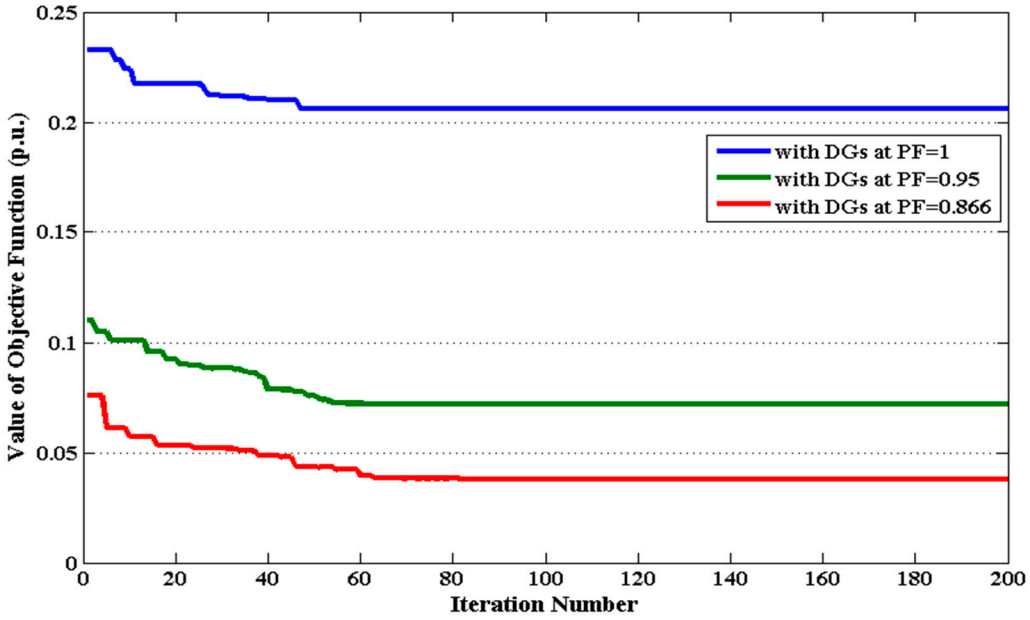

Figure 8. Convergence characteristics for Case 2 of the IEEE 33-bus system using QODELFA.

5.1.3. Case 3: Simultaneous Minimization of APL, VD, and VSI^{-1}

In this case, the minimization of APL (OF_1), VD (OF_2), and VSI^{-1} (OF_3) is simultaneously considered. Thus, the weighting factors in Equation (18) are taken as $\omega_1 = 1, \omega_2 = 0.65, \omega_3 = 0.35$, as in [32]. The QODELFA is implemented for three different values of power factor: Unity, 0.95 lag, and

0.866 lag. The results obtained from the proposed QODELFA are presented in Table 5 and compared to those from three other methods. It can be observed that, with unity power factor DGs (Case 3.1), the APL is minimized to 77.408 kW by using QODELFA, which is much less than that of 98.20 kW from SIMBO-Q [28], 97.10 kW from QOSIMBO-Q [28], and approximately the same as that from SFSA [32].

However, the VD and VSI^{-1} (in p.u.) obtained by QODELFA are not better than those obtained from both algorithms in [28].

Similar aspects can be remarked for Case 3.2 with DGs operating at PF = 0.95 lag when comparing the results obtained by QODELFA to those from methods in [28], where the ALP is reduced to 29.386 kW by the proposed algorithm, which is less than that of SIMBO-Q (32.40 kW) and QOSIMBO-Q (31.70 kW). The values of VD and VSI^{-1} obtained from QODELFA in this case are slightly higher than those obtained from both algorithms in [28].

Table 5. Results for the IEEE 33-bus RDS with simultaneous minimization of OF_1, OF_2, and OF_3.

Technique	Optimal Locations	Optimal Sizes (MW/MVAr)	APL (kW)	VD (p.u.)	VSI^{-1} (p.u.)	VSI (p.u.)	LR%	SD
Case 3.1: DGs with unity power factor (PF = 1)								
SIMBO-Q [28]	12 24 30	1.3482/0.0 1.3805/0.0 1.5000/0.0	98.20	0.00081	1.0370	0.9643	53.46	-
QOSIMBO-Q [28]	12 24 30	1.3465/0.0 1.3043/0.0 1.5000/0.0	97.10	0.00088	1.0383	0.9631	53.98	-
SFSA [32]	13 24 30	0.9647/0.0 1.1337/0.0 1.3018/0.0	77.410	0.00623	1.0891	0.9182	63.31	2.73E-07
QODELFA	**13** **24** **30**	**0.9647/0.0** **1.1334/0.0** **1.3017/0.0**	**77.408**	**0.00621**	**1.0891**	**0.9182**	**63.31**	**2.62E-10**
Case 3.2: DGs with lagging power factor (PF = 0.95)								
SIMBO-Q [28]	13 24 30	0.9429/0.3099 1.3271/0.4362 1.4429/0.4742	32.40	0.0003	1.0234	0.9771	84.74	-
QOSIMBO-Q [28]	13 24 30	0.8980/0.2952 1.3928/0.4578 1.4193/0.4665	31.70	0.0003	1.0235	0.9770	85.26	-
SFSA [32]	13 24 30	0.9174/0.3015 1.1463/0.3768 1.3157/0.4324	29.383	0.0007	1.0312	0.9697	86.07	1.47E-07
QODELFA	**13** **24** **30**	**0.9169/0.3013** **1.1466/0.3768** **1.3167/0.4327**	**29.386**	**0.0007**	**1.0311**	**0.9698**	**86.07**	**1.97E-09**
Case 3.3: DGs with lagging power factor (PF = 0.866)								
QODELFA	**13** **24** **30**	**0.7911/0.4567** **1.0411/0.5991** **1.2431/0.7178**	**15.498**	**0.0003**	**1.0242**	**0.9764**	**92.65**	**3.52E-08**

The sign "-" means unreported.

When the power factor is set to 0.866 lag (Case 3.3), the APL, VD, and VSI^{-1} are improved to 15.498 kW, 0.0003, and 1.0242 p.u., respectively. This verifies that better solutions can be achieved when choosing the best value of DGs' power factor.

Besides that, for all cases (3.1, 3.2, and 3.3), the robustness by the small SDs and the fast convergence of the proposed algorithm are validated as given in Table 5 and Figure 9, respectively. The voltage profiles for Case 3 of the IEEE 33-bus system are shown in Figure 10, where the voltages along the feeder are well enhanced for all subcases, especially for Case 3.3.

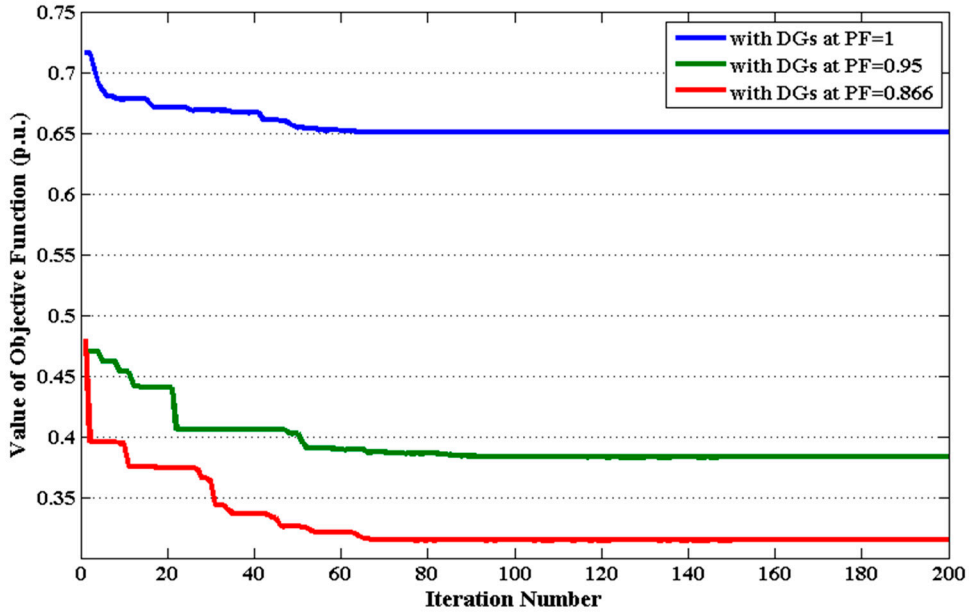

Figure 9. Convergence characteristics for Case 3 of the IEEE 33-bus system using QODELFA.

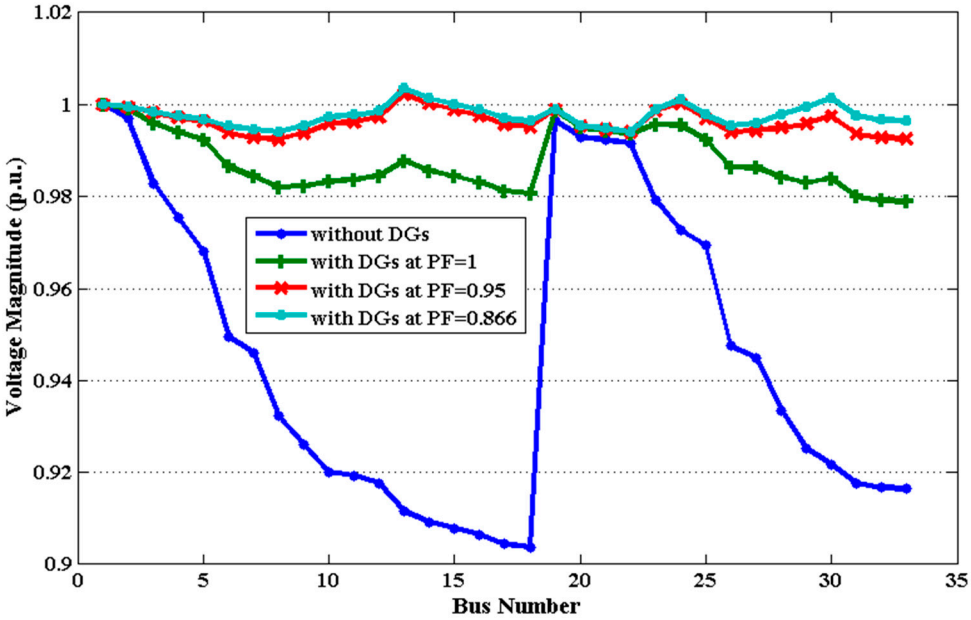

Figure 10. Voltage profile for Case 3 of the IEEE 33-bus system using QODELFA.

5.2. System 2: The IEEE 69-Bus

The load and line data of this RDS are taken from [39]. The base voltage and power are 12.66 kV and 100 MVA. The total active and reactive power loads are 3.80 MW and 2.69 MVAr, respectively. The base-case active and reactive power losses obtained from solving the BFSA-based load flow are 225 kW and 102.16 kVAr, respectively. The base-case values of the VD and (VSI^{-1}, VSI) are 0.09933 p.u. and (1.4635, 0.6833) p.u., respectively.

For this system, the QODELFA's optimal parameters are chosen as $PS = 50$, $cr = 0.9$, and $\beta = 1.8$ for all cases with $M = 200$.

5.2.1. Case 1: APL Minimization

The minimization of APL (OF_1) only, is considered in this case. Hence, the weighting factors in Equation (18) are taken as $\omega_1 = 1, \omega_2 = \omega_3 = 0$. By applying QODELFA for three different values of power factor: Unity, 0.95 lag, and 0.82 lag, the obtained results are presented in Table 6.

Table 6. Results for the IEEE 69-bus RDS with OF_1.

Technique	Optimal Locations	Optimal Sizes (MW/MVAr)	APL (kW)	VD (p.u.)	VSI^{-1} (p.u.)	VSI (p.u.)	LR%	SD
Case 1.1: DGs with unity power factor (PF = 1)								
QOSIMBO-Q [28]	9 18 61	0.8336/0.0 0.4511/0.0 1.5000/0.0	71.000	0.0071	1.1131	0.8984	68.44	-
MINLP [13]	11 17 61	0.5300/0.0 0.3800/0.0 1.7200/0.0	69.590	-	-	-	69.07	-
KHA [31]	12 22 61	0.4962/0.0 0.3113/0.0 1.7354/0.0	69.563	-	1.0887	0.9185	69.08	-
SFSA [32]	11 18 61	0.5273/0.0 0.3805/0.0 1.7198/0.0	69.428	0.00518	1.0886	0.9186	69.14	5.24E-08
QODELFA	**11** **18** **61**	**0.5267/0.0** **0.3806/0.0** **1.7189/0.0**	**69.426**	**0.00519**	**1.0887**	**0.9185**	**69.15**	**3.16E-10**
Case 1.2: DGs with lagging power factor (PF = 0.95)								
SIMBO-Q [28]	19 61 64	0.5656/0.1859 1.5000/0.4930 0.4220/0.1387	23.100	0.00075	1.0281	0.9727	89.73	-
QOSIMBO-Q [28]	17 61 64	0.5828/0.1916 1.5000/0.4930 0.4272/0.1404	22.800	0.00069	1.0266	0.9741	89.87	-
SFSA [32]	11 17 61	0.5435/0.1786 0.4132/0.1358 1.8728/0.6156	20.727	0.00033	1.0234	0.9772	90.79	6.51E-06
QODELFA	**11** **18** **61**	**0.5597/0.1839** **0.4172/0.1371** **1.8775/0.6171**	**20.716**	**0.00027**	**1.0235**	**0.9770**	**90.79**	**4.33E-08**
Case 1.3: DGs with lagging power factor (PF = 0.82)								
IA [39]	17 50 61	0.5100/0.3560 0.6798/0.4745 1.6999/1.1865	4.950	-	-	-	97.74	-
QODELFA	**11** **18** **61**	**0.4986/0.3480** **0.3762/0.2559** **1.6869/1.1774**	**4.286**	**0.00012**	**1.0234**	**0.9771**	**98.09**	**1.84E-05**

The sign "-" means unreported.

As it can be noted for cases 1.1 and 1.2, the active power loss is decreased from the base-case value (225 kW) to 69.426 kW with unity power factor DGs and to 20.716 with 0.95 lag power factor DGs by using the QODELFA. As demonstrated in Table 6 for each of cases 1.1 and 1.2, the values of APL obtained by applying QODELFA are better than those obtained by applying MINLP [13], QOSIMBO-Q [28], KHA [31], and SFSA [32]. The LR percentage is well increased to reach 98.09% when the power factor is set to 0.82 lag (Case 1.3).

This value is higher than that from the improved analytical method (IA) [39]. The APL obtained by applying QODELFA in all cases is obviously better than those from several algorithms in the literature, where the small SD of results is small enough to verify its robustness.

The convergence characteristics of QODELFA given in Figure 11 validate its effectiveness, where the proposed algorithm can quickly converge to the optimal solution for all cases (1.1, 1.2, and 1.3).

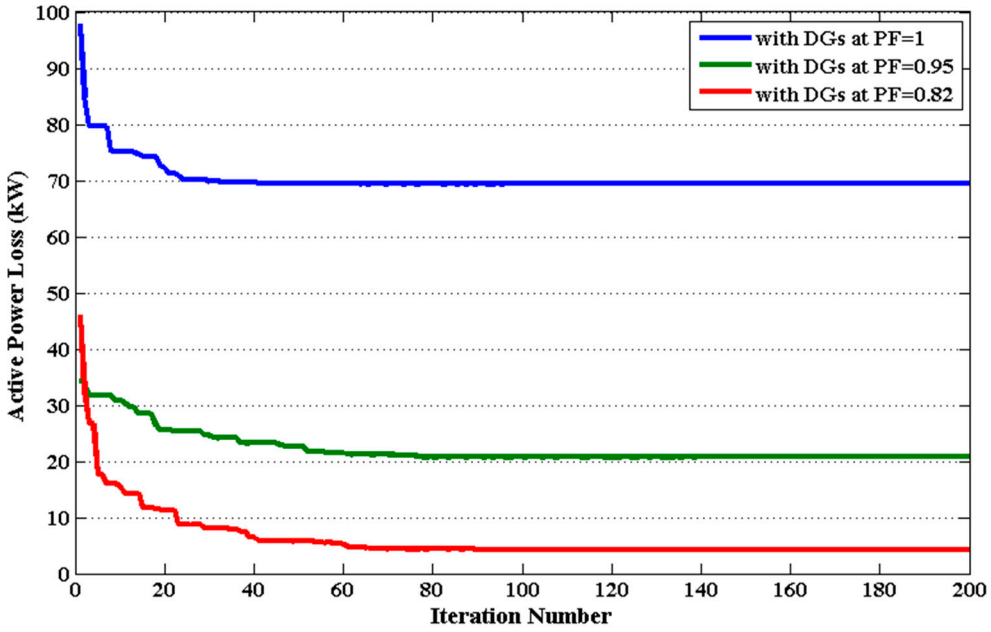

Figure 11. Convergence characteristics for Case 1 of the IEEE 69-bus system using QODELFA.

5.2.2. Case 2: Simultaneous Minimization of APL and VD

The simultaneous minimization of both APL (OF_1) and VD (OF_2) is considered in this case. Thus, as for the IEEE 33-bus system, the weighting factors in Equation (18) are taken as $\omega_1 = 0.5 = \omega_2 = 0.5, \omega_3 = 0$. The QODELFA is applied for three different values of power factor: Unity, 0.95 lag, and 0.82 lag. The results obtained by applying the proposed algorithm are outlined in Table 7.

It may be remarked that, the APL and VD are reduced to 72.154 kW and 0.00150 p.u. by using QODELFA with a unity power factor DGs (Case 2.1); to 20.806 kW and 0.00014 p.u. with a 0.95 lag power factor DGs (Case 2.2); and to 4.302 kW and 0.00010 p.u. with a 0.82 lag power factor DGs (Case 2.3). By comparing the results of cases 2.1 and 2.2 to those from both methods in [28], it might be easily noticed that the solutions provided by the QODELFA have a better compromise than those of SIMBO-Q and QOSIMBO-Q considering both OFs. As also demonstrated in Table 7, significant enhancement of APL as well as VD is obtained when the power factor is set to 0.82 lag (Case 2.3). The small SD of the obtained solutions is listed in Table 7 as well. In addition, the fast convergence of the proposed algorithm to the optimal solution for Case 2.1, 2.2, and 2.3 is depicted in Figure 12.

5.2.3. Case 3: Simultaneous Minimization of APL, VD, and VSI^{-1}

The simultaneous minimization of APL (OF_1), VD (OF_2) and VSI^{-1} (OF_3) is considered in this case. Accordingly, the weighting factors in Equation (18) are taken as $\omega_1 = 1, \omega_2 = 0.65, \omega_3 = 0.35$, as in [32]. The QODELFA is applied for three different values of power factor: Unity, 0.95 lag, and 0.82 lag. The results obtained from the proposed QODELFA are illustrated in Table 8 and compared to those from methods in [28,32].

Table 7. Results for the IEEE 69-bus RDS with simultaneous minimization of OF_1 and OF_2.

Technique	Optimal Locations	Optimal Sizes (MW/MVAr)	APL (kW)	VD (p.u.)	VSI^{-1} (p.u.)	VSI (p.u.)	LR%	SD
Case 2.1: DGs with unity power factor (PF = 1)								
SIMBO-Q [28]	16 59 61	0.7693/0.0 0.7233/0.0 1.4597/0.0	78.100	0.00100	-	-	65.29	-
QOSIMBO-Q [28]	18 59 61	0.6987/0.0 0.7037/0.0 1.5000/0.0	77.400	0.00100	-	-	65.6	-
QODELFA	**11** **20** **61**	**0.6616/0.0** **0.4554/0.0** **1.9201/0.0**	**72.154**	**0.00150**	**1.0535**	**0.9492**	**67.93**	**4.17E-05**
Case 2.2: DGs with lagging power factor (PF = 0.95)								
SIMBO-Q [28]	14 61 62	0.7976/0.2622 0.6549/0.2153 1.3615/0.4475	25.900	0.00020	-	-	88.48	-
QOSIMBO-Q [28]	14 61 64	0.8167/0.2685 1.5000/0.4930 0.4615/0.1517	24.600	0.00020	-	-	89.06	-
QODELFA	**11** **18** **61**	**0.5859/0.1926** **0.4359/0.1433** **1.9080/0.6272**	**20.806**	**0.00014**	**1.0235**	**0.9770**	**90.75**	**3.21E-04**
Case 2.3: DGs with lagging power factor (PF = 0.82)								
QODELFA	**11** **18** **61**	**0.5077/0.3544** **0.3875/0.2593** **1.6959/1.1837**	**4.302**	**0.00010**	**1.0234**	**0.9771**	**98.08**	**2.96E-04**

The sign "-" means unreported.

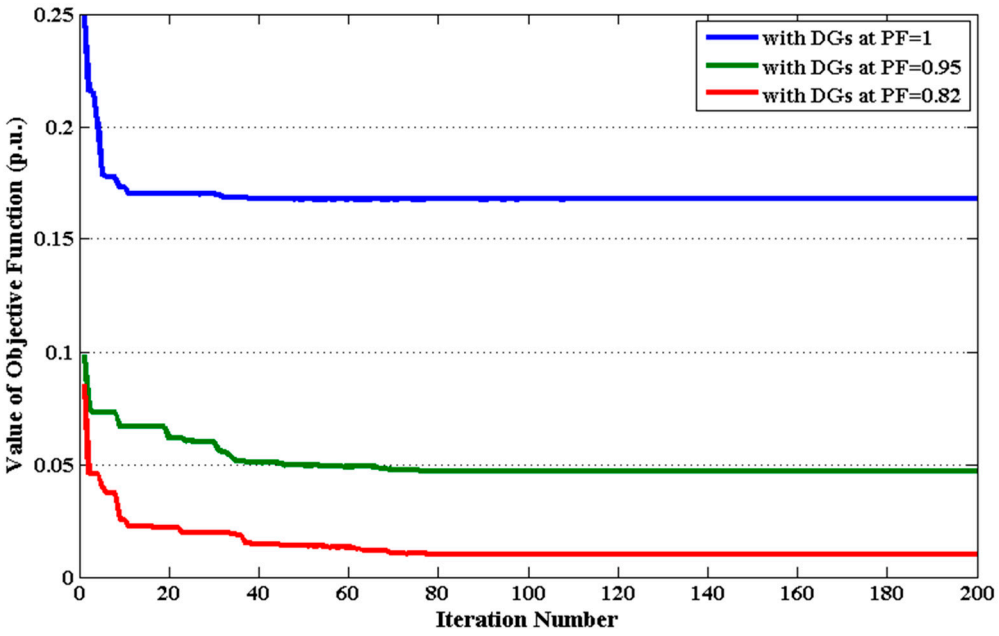

Figure 12. Convergence characteristics for Case 2 of the IEEE 69-bus system using QODELFA.

It may be observed that, by applying QODELFA with unity power factor DGs (Case 3.1), the APL is reduced to 72.295 kW, which is lower than that of 80.0 kW from SIMBO-Q [28], 79.70 kW from QOSIMBO-Q [28], and 72.445 kW from SFSA [32]. However, the VD and VSI^{-1} (in p.u.) obtained by QODELFA in this case are not better than those obtained from the algorithms in [28,32].

For Case 3.2 with DGs operating at PF = 0.95 lag, and by comparing the results obtained by QODELFA to those from methods in [28,32], it can be remarked that the APL is reduced to 20.774 kW by the proposed algorithm, which is less than that of SIMBO-Q (30.90 kW) and QOSIMBO-Q (25.70 kW), and the same as that of SFSA. Additionally, the value of VD obtained by QODELFA in this case (0.00015 p.u.) is better than the other three algorithms in [28,32]. Also, the VSI^{-1} values obtained from all compared algorithms are approximately the same in this case, which gives the proposed algorithm the advantage of providing better compromised solutions than the methods in [28], while almost the same performance is noted from both QODELFA and SFSA in [32].

Moreover, when the power factor is set to 0.82 lag (Case 3.3), the APL, VD, and VSI^{-1} are minimized to 4.297 kW, 0.00010, and 1.0234 p.u., respectively. This proves that when selecting the best value of DGs' power factor, better solutions can be achieved.

Table 8. Results for the IEEE 69-bus RDS with simultaneous minimization of OF_1, OF_2 and OF_3.

Technique	Optimal Locations	Optimal Sizes (MW/MVAr)	APL (kW)	VD (p.u.)	VSI^{-1} (p.u.)	VSI (p.u.)	LR%	SD
Case 3.1: DGs with unity power factor (PF = 1)								
SIMBO-Q [28]	15 61 62	0.7722/0.0 1.3526/0.0 0.8232/0.0	80.000	0.00070	1.0235	0.9770	64.44	-
QOSIMBO-Q [28]	15 61 63	0.7754/0.0 1.4385/0.0 0.7235/0.0	79.700	0.00070	1.0237	0.9770	64.58	-
SFSA [32]	11 19 61	0.5703/0.0 0.4661/0.0 1.9674/0.0	72.445	0.00143	1.0485	0.9537	67.80	3.80E-05
QODELFA	**11** **20** **61**	**0.6294/0.0** **0.4386/0.0** **1.9537/0.0**	**72.295**	**0.00150**	**1.0499**	**0.9525**	**67.87**	**2.12E-05**
Case 3.2: DGs with lagging power factor (PF = 0.95)								
SIMBO-Q [28]	15 56 62	0.5380/0.1768 1.2817/0.4213 1.5000/0.4930	30.900	0.00020	1.0233	0.9772	86.27	-
QOSIMBO-Q [28]	14 60 61	0.8276/0.2720 0.5339/0.1755 1.5000/0.4930	25.700	0.00020	1.0234	0.9771	88.58	-
SFSA [32]	11 18 61	0.5804/0.1908 0.4344/0.1428 1.8992/0.6242	20.774	0.00016	1.0234	0.9772	90.77	1.10E-04
QODELFA	**11** **18** **61**	**0.5797/0.1905** **0.4340/0.1426** **1.9013/0.6249**	**20.774**	**0.00015**	**1.0235**	**0.9770**	**90.77**	**1.24E-04**
Case 3.3: DGs with lagging power factor (PF = 0.82)								
QODELFA	**11** **18** **61**	**0.5058/0.3531** **0.3859/0.2589** **1.6939/1.1823**	**4.297**	**0.00010**	**1.0234**	**0.9771**	**98.09**	**2.27E-04**

The sign "-" means unreported.

Besides that, as demonstrated in Table 8 and Figure 13 for all cases (3.1, 3.2, and 3.3), the effectiveness of the proposed algorithm is verified by the small SDs and the fast convergence to the optimal solutions as well. As illustrated in Figure 14, the voltages at all buses of the IEEE 69-bus system for Case 3 are well enhanced, where the most improvement is achieved for Case 3.3.

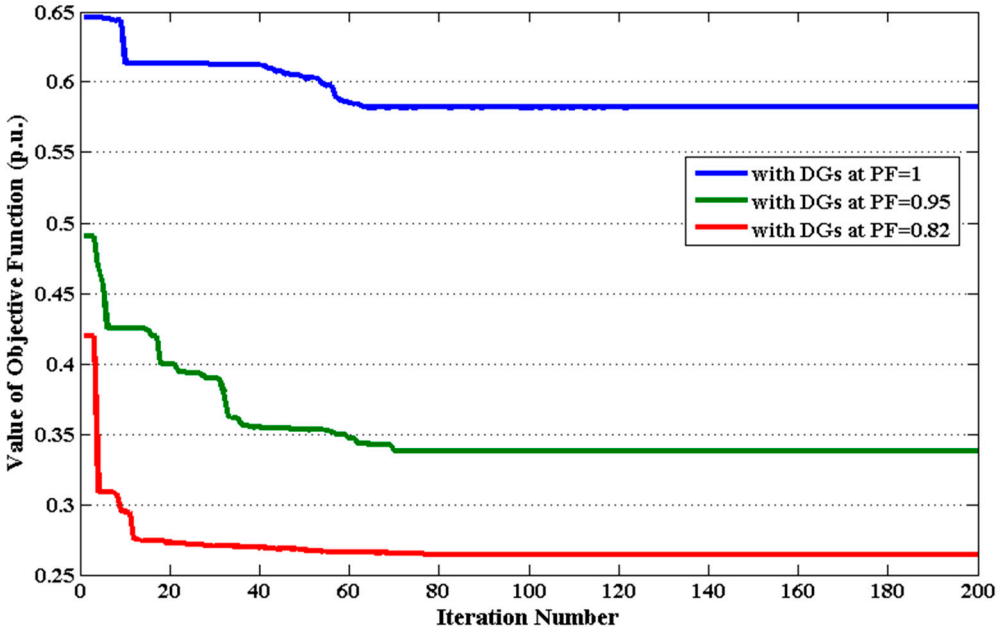

Figure 13. Convergence characteristics for Case 3 of the IEEE 69-bus system using QODELFA.

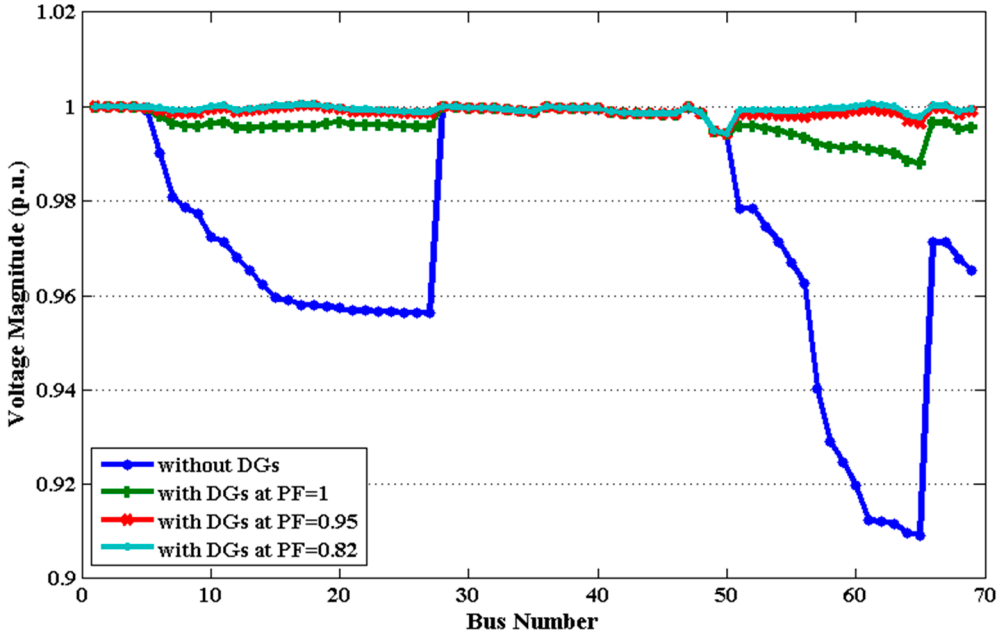

Figure 14. Voltage profile for Case 3 of the IEEE 69-bus system using QODELFA.

5.3. System 3: The IEEE 118-Bus

The load and line data of this large-scale RDS are taken from [41] where the bus numbers are rearranged. The base voltage and power are 11 kV and 100 MVA. The total active and reactive power loads are 22.710 MW and 17.041 MVAr, respectively.

The base-case active and reactive power losses obtained from solving the BFSA-based load flow are 1297.95 kW and 978.54 kVAr, respectively. The base-case values of the VD and (VSI^{-1}, VSI) are 0.35764 p.u. and (1.7552, 0.5697) p.u., respectively. For this system, the QODELFA's optimal parameters are selected as $PS = 50$, $cr = 0.9$, and $\beta = 1.8$ for all cases with $M = 300$.

5.3.1. Case 1: APL Minimization

The weighting factors in Equation (18) are taken as $\omega_1 = 1, \omega_2 = \omega_3 = 0$; in this case as only the APL minimization (OF_1) is considered.

The QODELFA is implemented for unity, 0.866 lag, and 0.82 lag power factors. The results are listed in Table 9. It may be clearly observed that the APL is decreased from the base-case value (1297.95 kW) to 518.653 kW with unity power factor DGs (Case 1.1) by using the proposed algorithm. From the comparison outlined in Table 9, the APL obtained by applying QODELFA is better than that of 576.182 kW from QOTLBO [29], 574.710 kW from KHA [31], and 525.277 kW from SFSA [32].

The APL is more reduced in Case 1.2 (when the power factor is set to 0.866 lag) by implementing the proposed QODELFA, where it reaches 148.931 kW. This value is lower than that of 312.661 kW from KHA [31], and 155.159 kW from SFSA [32].

The most significant LR value is reached when setting the power factor to 0.82 lag (Case 1.3), where it is increased to 89.77% by using the proposed algorithm. Table 9 and Figure 15 respectively depict the small values of SD and the fast convergence to the optimal solutions for all cases, which indicates the robustness and effectiveness of the QODELFA.

5.3.2. Case 2: Simultaneous Minimization of APL and VD

In this case, the weighting factors in Equation (18) are taken as $\omega_1 = 0.65, \omega_2 = 0.35, \omega_3 = 0$ in order to achieve the best results, since the simultaneous minimization of both APL (OF_1) and VD (OF_2) is considered. Three different values of power factor: Unity, 0.866 lag, and 0.82 lag are defined as the subcases for the QODELFA's implementation.

It may be noted from the results shown in Table 10 obtained by applying the proposed algorithm that the APL and VD are decreased to 536.134 kW and 0.0365 p.u. with unity power factor DGs (Case 2.1); to 149.215 kW and 0.0067 p.u. with 0.866 lag power factor DGs (Case 2.2); and to 134.049 kW and 0.0064 p.u. with 0.82 lag power factor DGs (Case 2.3).

As presented in Table 10, strong improvements of APL and VD are obtained in the last subcase. The SD of the results is also given in Table 10. Moreover, the fast convergence of QODELFA to the optimal solution for Case 2.1, 2.2, and 2.3 is demonstrated in Figure 16.

5.3.3. Case 3: Simultaneous Minimization of APL, VD, and VSI^{-1}

The weighting factors in Equation (18) are taken as $\omega_1 = 1, \omega_2 = 0.65, \omega_3 = 0.35$, as in [32], where the simultaneous minimization of APL (OF_1), VD (OF_2,), and VSI^{-1} (OF_3) is considered.

The QODELFA is applied for three different values of power factor: Unity, 0.866 unity, and 0.82 lag. It may be noted from the results listed in Table 11 that, by applying QODELFA with unity power factor DGs (Case 3.1), the APL, VD, and VSI^{-1} are decreased to 554.682 kW, 0.0297 p.u., and 1.1250 p.u., respectively, which are better than those from SFSA [32] and SOS [32]. The obtained results from QODELFA are also better than those from QOTLBO [29], except for the VD value. Nevertheless, the QODELFA's overall solutions have a better compromise than those of QOTLBO considering the three OFs together.

By comparing the results obtained by QODELFA to those from SFSA [32] for Case 3.2 with DGs operating at PF = 0.866 lag, it can be noticed that the proposed algorithm's solutions provide a better compromise regarding APL (156.142 kW), VD (0.0067 p.u.), and VSI^{-1} (1.1024 p.u.) than the solutions of 176.969 kW, 0.00852 p.u., and 1.0978 p.u., respectively, from SFSA [32].

Table 9. Results for the IEEE 118-bus RDS with OF_1.

Technique	Optimal Locations	Optimal Sizes (MW/MVAr)	APL (kW)	VD (p.u.)	VSI^{-1} (p.u.)	VSI (p.u.)	LR%	SD
Case 1.1: DGs with unity power factor (PF = 1)								
QOTLBO [29]	24 42 47 74 78 94 108	1.2463/0.0 0.7322/0.0 3.5392/0.0 2.6792/0.0 1.2483/0.0 1.0865/0.0 3.2432/0.0	576.182	0.0629	1.2093	0.8269	55.61	-
KHA [31]	48 53 74 80 96 109 112	1.7242/0.0 1.3356/0.0 1.8623/0.0 1.8653/0.0 1.6631/0.0 1.9473/0.0 1.1848/0.0	574.710	-	1.2433	0.8043	55.73	-
SFSA [32]	21 42 50 71 81 97 110	1.3757/0.0 1.1997/0.0 2.7418/0.0 2.8915/0.0 1.7025/0.0 1.3321/0.0 2.6674/0.0	525.277	0.0612	1.2090	0.8271	59.53	6.40E-03
QODELFA	**20** **39** **47** **73** **80** **90** **110**	**1.7908/0.0** **2.7341/0.0** **1.8329/0.0** **2.4034/0.0** **1.7505/0.0** **2.2945/0.0** **2.7998/0.0**	**518.653**	**0.0578**	**1.2129**	**0.8245**	**60.04**	**7.50E-03**
Case 1.2: DGs with lagging power factor (PF = 0.866)								
KHA [31]	43 51 69 73 88 108 109	1.9726/1.1389 1.9849/1.1460 1.7929/1.0351 1.8551/1.0710 1.8975/1.0955 1.9905/1.1492 1.9951/1.1519	312.661	-	1.1393	0.8777	75.91	-
SFSA [32]	21 40 50 71 80 96 110	1.9351/1.1174 2.0810/1.2016 3.1301/1.8074 2.8920/1.6699 2.0541/1.1861 1.3859/0.8003 3.2306/1.8654	155.159	0.00861	1.1015	0.9078	88.05	1.10E-02
QODELFA	**20** **39** **46** **74** **85** **90** **110**	**1.8771/1.0839** **3.0909/1.7847** **2.1775/1.2573** **2.3591/1.3621** **1.7023/0.9829** **2.4516/1.4156** **3.1123/1.7971**	**148.931**	**0.00860**	**1.1024**	**0.9071**	**88.53**	**2.17E-02**
Case 1.3: DGs with lagging power factor (PF = 0.82)								
QODELFA	**20** **39** **46** **74** **85** **91** **110**	**1.7850/1.2459** **2.9683/2.0719** **2.0693/1.4443** **2.2927/1.4828** **1.7000/1.0798** **2.1408/1.4943** **2.9738/2.0758**	**132.787**	**0.00790**	**1.1033**	**0.9064**	**89.77**	**3.42E-03**

The sign "-" means unreported.

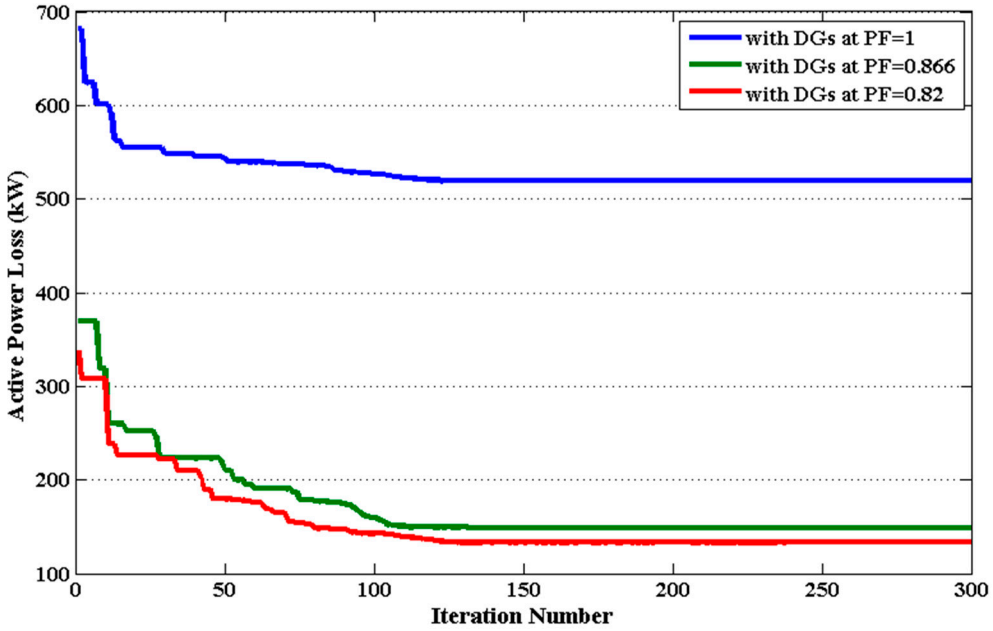

Figure 15. Convergence characteristics for Case 1 of the IEEE 118-bus system using QODELFA.

When the power factor is set to 0.82 lag (Case 3.3), the APL, VD, and VSI^{-1} are well minimized to 134.978 kW, 0.006 p.u., and 1.1009 p.u., respectively. Table 11 and Figure 17 verify the effectiveness as well as the robustness of the proposed algorithm for all cases (3.1, 3.2, and 3.3) by demonstrating, respectively, the small SDs and the fast convergence.

The voltage profiles for Case 3 of the IEEE 118-bus system depicted in Figure 18 indicate the significant enhancement of all bus voltages for all subcases, especially for Case 3.3.

Table 10. Results for the IEEE 118-bus RDS with simultaneous minimization of OF_1 and OF_2.

Technique	Optimal Locations	Optimal Sizes (MW/MVAr)	APL (kW)	VD (p.u.)	VSI^{-1} (p.u.)	VSI (p.u.)	LR%	SD
Case 2.1: DGs with unity power factor (PF = 1)								
QODELFA	20 39 47 73 80 90 110	2.0856/0.0 3.3381/0.0 2.1249/0.0 2.7940/0.0 2.0369/0.0 2.6069/0.0 3.1877/0.0	536.134	0.0365	1.1641	0.8590	58.69	6.74E-03
Case 2.2: DGs with lagging power factor (PF = 0.866)								
QODELFA	20 39 47 74 85 90 110	2.0187/1.1656 3.2905/1.9000 2.0615/1.1903 2.4092/1.3911 1.7437/1.0069 2.5473/1.4709 3.1775/1.8348	149.215	0.0067	1.1044	0.9055	88.50	5.39E-03
Case 2.3: DGs with lagging power factor (PF = 0.82)								
QODELFA	20 39 46 74 85 91 110	1.8988/1.3254 3.1073/2.1689 2.2465/1.5680 2.3442/1.5137 1.7033/1.1081 2.2008/1.5361 3.0356/2.1189	134.049	0.0064	1.1045	0.9054	89.67	3.68E-03

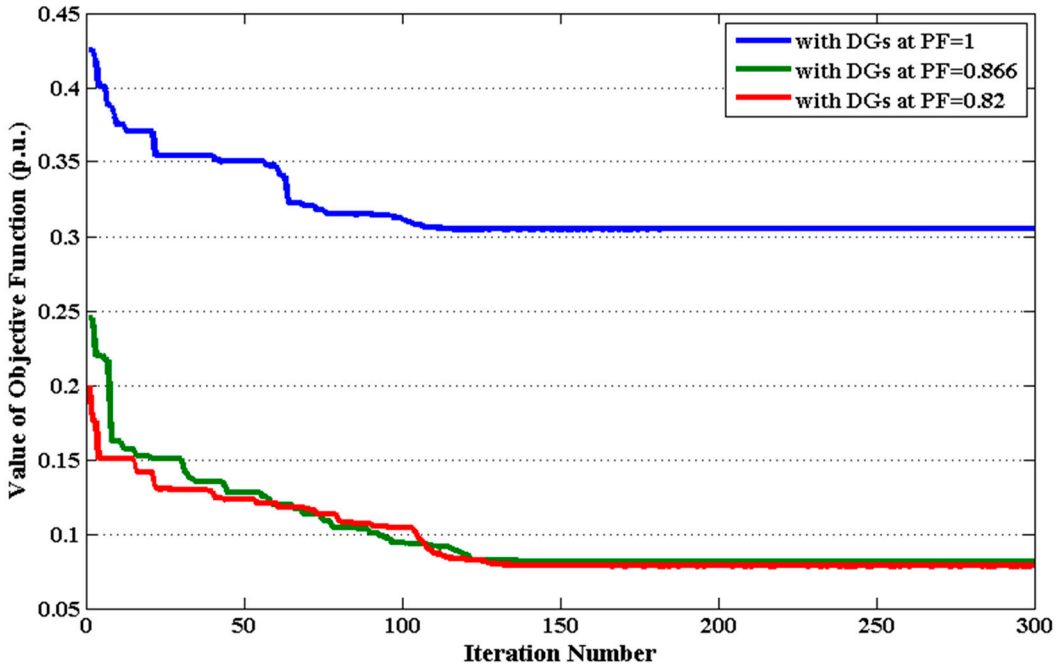

Figure 16. Convergence characteristics for Case 2 of the IEEE 118-bus system using QODELFA.

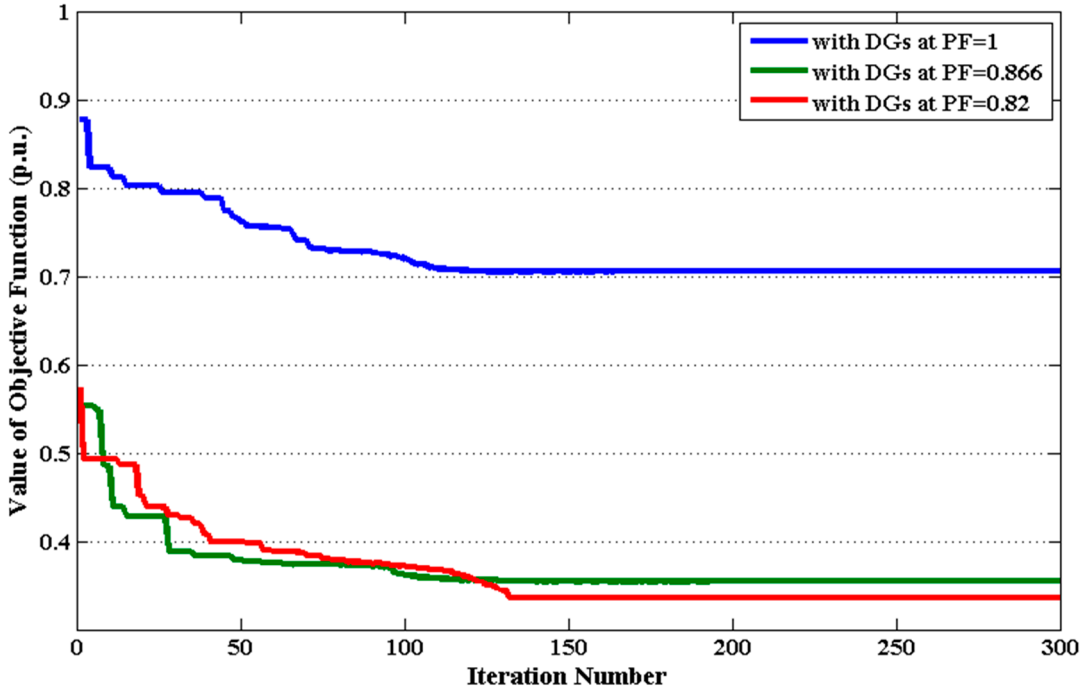

Figure 17. Convergence characteristics for Case 3 of the IEEE 118-bus system using QODELFA.

Table 11. Results for the IEEE 118-bus RDS with simultaneous minimization of OF_1, OF_2, and OF_3.

Technique	Optimal Locations	Optimal Sizes (MW/MVAr)	APL (kW)	VD (p.u.)	VSI^{-1} (p.u.)	VSI (p.u.)	LR%	SD
Case 3.1: DGs with unity power factor (PF = 1)								
QOTLBO [29]	43	1.5880/0.0	677.588	0.02330	1.1372	0.8794	47.80	-
	49	3.8459/0.0						
	54	0.9852/0.0						
	74	3.1904/0.0						
	80	3.1632/0.0						
	94	1.9527/0.0						
	111	3.6013/0.0						
SFSA [32]	19	2.0313/0.0	564.104	0.03085	1.1420	0.8757	56.54	6.20E-03
	41	1.9135/0.0						
	49	4.0113/0.0						
	73	2.7996/0.0						
	79	3.0734/0.0						
	96	2.0861/0.0						
	108	3.8194/0.0						
SOS [32]	18	3.1920/0.0	561.000	0.0675	1.2032	0.8311	56.78	-
	39	2.7580/0.0						
	48	1.2360/0.0						
	66	1.4450/0.0						
	74	2.0650/0.0						
	80	1.9480/0.0						
	110	2.6780/0.0						
QODELFA	**20**	**2.1256/0.0**	**554.682**	**0.0297**	**1.1250**	**0.8889**	**57.26**	**6.74E-03**
	39	**3.8797/0.0**						
	47	**2.3173/0.0**						
	73	**2.8518/0.0**						
	80	**2.0957/0.0**						
	91	**2.4212/0.0**						
	110	**3.2376/0.0**						
Case 3.2: DGs with lagging power factor (PF = 0.866)								
SFSA [32]	19	1.8454/1.0656	176.969	0.00852	1.0978	0.9109	86.37	1.30E-02
	39	2.2060/1.2738						
	50	3.6561/2.1111						
	74	2.2638/1.3071						
	80	2.4474/1.4132						
	90	2.0355/1.1753						
	108	3.4768/2.0076						
QODELFA	**18**	**2.4594/1.4201**	**156.142**	**0.00670**	**1.1024**	**0.9071**	**87.97**	**2.21E-02**
	39	**3.3315/1.9237**						
	47	**2.1185/1.2233**						
	73	**2.4898/1.4377**						
	80	**1.8385/1.0616**						
	91	**2.3071/1.3322**						
	110	**3.1879/1.8407**						
Case 3.3: DGs with lagging power factor (PF = 0.82)								
QODELFA	**20**	**1.9294/1.3467**	**134.978**	**0.00600**	**1.1009**	**0.9083**	**89.60**	**1.84E-02**
	39	**3.1467/2.1964**						
	46	**2.3361/1.6306**						
	74	**2.3503/1.5174**						
	85	**1.7077/1.1109**						
	91	**2.2096/1.5423**						
	110	**3.0441/2.1248**						

The sign "-" means unreported.

By implementing the QODELFA on the benchmark functions as well as the OPDG problem, its advantages can be concluded as follows:

1. Two main mechanisms are combined to construct the proposed QODELFA; the former finds the global optimum solution using DE, whereas, the latter implements a local permutation using LF. Furthermore, the initial population of the combined DELF is generated by applying the QOBL concept, which consequently increases the diversity and exploration of the initial solutions. As a result, the implementation of the proposed QODELFA ensures the convergence towards the optimum rapidly and reliably. In addition, the elite solutions are elected in each generation, which guarantees the efficient and flexible flow of solutions to the optimal region inside the search space.
2. The obtained results presented in this paper show that the SDs are quite small. Hence, the proposed algorithm's performance stability and robustness are validated.
3. The effectiveness of the QODELFA is also verified by demonstrating the convergence characteristics of the proposed algorithm as given in this paper. Apparently, the optimal solutions are obtained with a small number of iterations.

Additionally, the disadvantages are summarized:

1. The computational time for QODELFA is slightly more than some original algorithms discussed in the literature and the paper. This is mainly because of the combined framework of three powerful search mechanisms together; namely, QOBL, DE, and LF, in addition to the implementation of crossover and selection many times during the execution of the proposed algorithm. Nevertheless, using a relatively more powerful computer can overcome this problem. Also, a slight additional computational time can be neglected when much better solutions are obtained.
2. The proposed algorithm has been tested using well-known benchmark functions, including, many minima, bowl-shaped, valley-shaped, and other difficult objective functions besides the OPDG problem solved in this paper. Hence, it is recommended here, to further investigate the performance of the algorithm in other engineering applications.

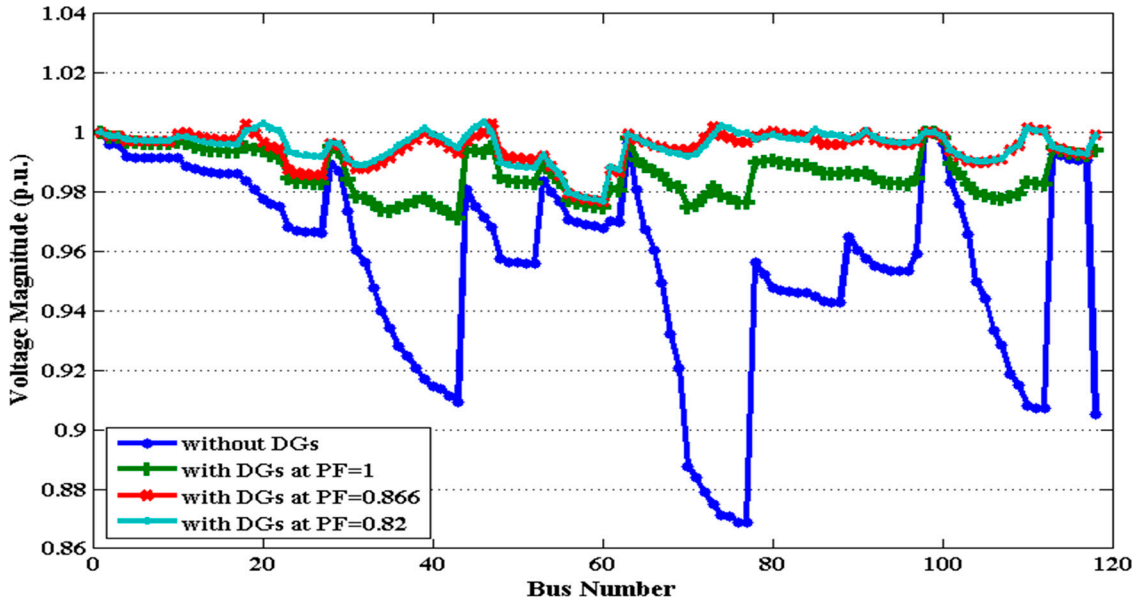

Figure 18. Voltage profile for Case 3 of the IEEE 118-bus system using QODELFA.

6. Conclusions

The proposed QODELFA has been applied to solve the OPDG problem in RDSs by taking three objective functions under consideration, which are the active power loss minimization, the voltage profile improvement, and the voltage stability enhancement. Different combinations of those objective functions by using the weighted sum method have been studied while satisfying different operational

constraints. The effectiveness of the proposed QODELFA for solving the OPDG problem has been verified on the IEEE 33-bus, 69-bus, and 118-bus systems. For each system, three values of DGs' power factor have been included in the analysis. The performed comparisons between the proposed QODELFA and several existing methods from the literature for the three test systems have depicted that the proposed algorithm has better performance than many of the previous methods for most of the studied cases, particularly for the large-scale IEEE 118-bus system. Moreover, the results have signified that the proper selection of the DGs' power factor plays an important role in achieving the best solutions regarding the three studied objective functions. Additionally, the robustness and effectiveness of the proposed algorithm in solving the OPDG problem have been validated by depicting the fast convergence and small standard deviations for all cases. As a result, the QODELFA can be suggested as a powerful method for solving the OPDG problem.

Author Contributions: R.J.M. and N.F.A. did the methodology, simulation, and validation. R.J.M. did the analysis and wrote the paper. Conceptualization, R.J.M, Y.S., and N.F.A.; software, R.J.M., Y.S., and N.F.A.; investigation, R.J.M. and N.F.A.; resources, R.J.M., Y.S., and N.F.A.; data curation, R.J.M., Y.S., N.F.A. and H.H.A.; writing—original draft preparation, R.J.M.; writing—reviewing and editing, R.J.M., Y.S., N.F.A., H.H.A., P.S. and M.S.-k.; visualization, R.J.M., Y.S., N.F.A., H.H.A., P.S. and M.S.-k.; supervision, Y.S. and P.S.; project administration, Y.S.; funding acquisition, Y.S. and H.H.A.

Funding: This work was supported in part by the National Natural Science Foundation of China under Grant 61673161, and in part by the Natural Science Foundation of Jiangsu Province of China under Grant BK20161510.

Conflicts of Interest: The authors declare no conflict of interest.

References

1. Sultana, U.; Khairuddin, A.B.; Aman, M.M.; Mokhtar, A.S.; Zareen, N. A review of optimum DG placement based on minimization of power losses and voltage stability enhancement of distribution system. *Renew. Sustain. Energy Rev.* **2016**, *63*, 363–378. [CrossRef]
2. Napis, N.F.; Khatib, T.; Hassan, E.E.; Sulaima, M.F. An improved method for reconfiguring and optimizing electrical active distribution network using evolutionary particle swarm optimization. *Appl. Sci.* **2018**, *8*, 804. [CrossRef]
3. Yaprakdal, F.; Baysal, M.; Anvari-Moghaddam, A. Optimal operational scheduling of reconfigurable microgrids in presence of renewable energy sources. *Energies* **2019**, *12*, 1858. [CrossRef]
4. Abd El-salam, M.F.; Beshr, E.; Eteiba, M.B. A new hybrid technique for minimizing power losses in a distribution system by optimal sizing and siting of distributed generators with network reconfiguration. *Energies* **2018**, *11*, 3351. [CrossRef]
5. Zhang, X.; Yang, J.; Wang, W.; Jing, T.; Zhang, M. Optimal operation analysis of the distribution network comprising a micro energy grid based on an improved grey wolf optimization algorithm. *Appl. Sci.* **2018**, *8*, 923. [CrossRef]
6. Aman, M.M.; Jasmon, G.B.; Mokhlis, H.; Bakar, A.H.A. Optimal placement and sizing of a DG based on a new power stability index and line losses. *Int. J. Electr. Power Energy Syst.* **2012**, *43*, 1296–1304. [CrossRef]
7. Murty, V.V.S.N.; Kumar, A. Optimal placement of DG in radial distribution systems based on new voltage stability index under load growth. *Int. J. Electr. Power Energy Syst.* **2015**, *69*, 246–256. [CrossRef]
8. Kumar, A.; Vijay Babu, P.; Murty, V.V.S.N. Distributed generators allocation in radial distribution systems with load growth using loss sensitivity approach. *J. Inst. Eng. India Ser. B* **2017**, *98*, 275–287. [CrossRef]
9. Murty, V.V.S.N.; Kumar, A. Comparison of optimal DG allocation methods in radial distribution systems based on sensitivity approaches. *Int. J. Electr. Power Energy Syst.* **2013**, *53*, 450–467. [CrossRef]
10. Viral, R.; Khatod, D.K. An analytical approach for sizing and siting of DGs in balanced radial distribution networks for loss minimization. *Int. J. Electr. Power Energy Syst.* **2015**, *67*, 191–201. [CrossRef]
11. Atwa, Y.M.; El-Saadany, E.F.; Salama, M.M.A.; Seethapathy, P. Optimal renewable resources mix for distribution system energy loss minimization. *IEEE Trans. Power Syst.* **2010**, *25*, 360–370. [CrossRef]
12. Khalesi, N.; Rezaei, N.; Haghifam, M.R. DG allocation with application of dynamic programming for loss reduction and reliability improvement. *Int. J. Electr. Power Energy Syst.* **2011**, *33*, 288–295. [CrossRef]
13. Kaur, S.; Kumbhar, G.; Sharma, J. A MINLP technique for optimal placement of multiple DG units in distribution systems. *Int. J. Electr. Power Energy Syst.* **2014**, *63*, 609–617. [CrossRef]

14. Shaaban, M.F.; Atwa, Y.M.; El-Saadany, E.F. DG allocation for benefit maximization in distribution networks. *IEEE Trans. Power Syst.* **2013**, *28*, 639–649. [CrossRef]
15. Ganguly, S.; Samajpati, D. Distributed generation allocation on radial distribution networks under uncertainties of load and generation using genetic algorithm. *IEEE Trans. Sustain. Energy* **2015**, *6*, 688–697. [CrossRef]
16. Ganguly, S.; Samajpati, D. Distributed generation allocation with on-load tap changer on radial distribution networks using adaptive genetic algorithm. *Appl. Soft Comput.* **2017**, *59*, 45–67. [CrossRef]
17. El-Zonkoly, A.M. Optimal placement of multi-distributed generation units including different load models using particle swarm optimization. *Swarm Evol. Comput.* **2011**, *1*, 50–59. [CrossRef]
18. Kansal, S.; Kumar, V.; Tyagi, B. Optimal placement of different type of DG sources in distribution networks. *Int. J. Electr. Power Energy Syst.* **2013**, *53*, 752–760. [CrossRef]
19. HassanzadehFard, H.; Jalilian, A. Optimal sizing and location of renewable energy based DG units in distribution systems considering load growth. *Int. J. Electr. Power Energy Syst.* **2018**, *101*, 356–370. [CrossRef]
20. Abu-Mouti, F.S.; El-Hawary, M.E. Optimal distributed generation allocation and sizing in distribution systems via artificial bee colony algorithm. *IEEE Trans. Power Deliv.* **2011**, *26*, 2090–2101. [CrossRef]
21. Niknam, T.; Taheri, S.I.; Aghaei, J.; Tabatabaei, S.; Nayeripour, M. A modified honey bee mating optimization algorithm for multiobjective placement of renewable energy resources. *Appl. Energy* **2011**, *88*, 4817–4830. [CrossRef]
22. Abdul Kadir, A.F.; Mohamed, A.; Shareef, H.; Ibrahim, A.A.; Khatib, T.; Elmenreich, W. An improved gravitational search algorithm for optimal placement and sizing of renewable distributed generation units in a distribution system for power quality enhancement. *J. Renew. Sustain. Energy* **2014**, *6*, 033112. [CrossRef]
23. Das, B.; Mukherjee, V.; Das, D. DG placement in radial distribution network by symbiotic organisms search algorithm for real power loss minimization. *Appl. Soft Comput.* **2016**, *49*, 920–936. [CrossRef]
24. Moradi, M.H.; Abedini, M. A combination of genetic algorithm and particle swarm optimization for optimal DG location and sizing in distribution systems. *Int. J. Electr. Power Energy Syst.* **2012**, *34*, 66–74. [CrossRef]
25. Nowdeh, S.A.; Davoudkhani, I.F.; Moghaddam, M.J.H.; Najmi, E.S.; Abdelaziz, A.Y.; Ahmadi, A.; Razavi, S.E.; Gandoman, F.H. Fuzzy multi-objective placement of renewable energy sources in distribution system with objective of loss reduction and reliability improvement using a novel hybrid method. *Appl. Soft Comput.* **2019**, *77*, 761–779. [CrossRef]
26. Kumar, S.; Mandal, K.K.; Chakraborty, N. Optimal DG placement by multi-objective opposition based chaotic differential evolution for techno-economic analysis. *Appl. Soft Comput.* **2019**, *78*, 70–83. [CrossRef]
27. Kayalvizhi, S.; Vinod Kumar, D.M. Optimal planning of active distribution networks with hybrid distributed energy resources using grid-based multi-objective harmony search algorithm. *Appl. Soft Comput.* **2018**, *67*, 387–398.
28. Sharma, S.; Bhattacharjee, S.; Bhattacharya, A. Quasi-oppositional swine influenza model based optimization with quarantine for optimal allocation of DG in radial distribution network. *Int. J. Electr. Power Energy Syst.* **2016**, *74*, 348–373. [CrossRef]
29. Sultana, S.; Roy, P.K. Multi-objective quasi-oppositional teaching learning based optimization for optimal location of distributed generator in radial distribution systems. *Int. J. Electr. Power Energy Syst.* **2014**, *63*, 534–545. [CrossRef]
30. Injeti, S.K.; Kumar, N.P. A novel approach to identify optimal access point and capacity of multiple DGs in a small, medium and large scale radial distribution systems. *Int. J. Electr. Power Energy Syst.* **2013**, *45*, 142–151. [CrossRef]
31. Sultana, S.; Roy, P.K. Krill herd algorithm for optimal location of distributed generator in radial distribution system. *Appl. Soft Comput.* **2016**, *40*, 391–404. [CrossRef]
32. Nguyen, T.P.; Vo, D.N. A novel stochastic fractal search algorithm for optimal allocation of distributed generators in radial distribution systems. *Appl. Soft Comput.* **2018**, *70*, 773–796. [CrossRef]
33. Storn, R.; Price, K. Differential evolution – A simple and efficient heuristic for global optimization over continuous spaces. *J. Glob. Optim.* **1997**, *11*, 341–359. [CrossRef]
34. Yang, X.S.; Deb, S. Cuckoo search via Lévy flights. In Proceedings of the 2009 World Congress on Nature & Biologically Inspired Computing (NaBIC), Coimbatore, India, 9–11 December 2009; pp. 210–214.

35. Tizhoosh, H.R. Opposition-based learning: A new scheme for machine intelligence. In Proceedings of the International Conference on Computational Intelligence for Modelling, Control and Automation and International Conference on Intelligent Agents, Web Technologies and Internet Commerce (CIMCA-IAWTIC'06), Vienna, Austria, 28–30 November 2005; pp. 1–7.
36. Simon, D.; Ergezer, M.; Du, D. Oppositional Biogeography-Based Optimization. Available online: http://embeddedlab.csuohio.edu/BBO/ (accessed on 3 June 2019).
37. Surjanovic, S.; Bingham, D. Virtual Library of Simulation Experiments: Test Functions and Datasets. Available online: https://www.sfu.ca/~{}ssurjano/index.html (accessed on 1 June 2019).
38. Reddy, V.U.; Manohar, T.G. A two stage approach: Capacitor placement for loss reduction in radial distribution system. In Proceedings of the 2012 11th International Conference on Environment and Electrical Engineering, Venice, Italy, 18–25 May 2012; pp. 555–558.
39. Hung, D.Q.; Mithulananthan, N. Multiple distributed generator placement in primary distribution networks for loss reduction. *IEEE Trans. Ind. Electron.* **2013**, *60*, 1700–1708. [CrossRef]
40. Zulpo, R.S.; Leborgne, R.C.; Bretas, A.S. Optimal siting and sizing of distributed generation through power losses and voltage deviation. In Proceedings of the 2014 16th International Conference on Harmonics and Quality of Power (ICHQP), Bucharest, Romania, 25–28 May 2014; pp. 871–875.
41. El-Fergany, A.A.; Abdelaziz, A.Y. Capacitor allocations in radial distribution networks using cuckoo search algorithm. *IET Gener. Transm. Distrib.* **2014**, *8*, 223–232. [CrossRef]